

Where is the Carbon? Spatially Mapping Organic Carbon on the Seafloor in the Eastern Shore
Islands, Nova Scotia, Canada

by

Catherine E. Brennan

Submitted in partial fulfillment of the requirements for the degree of Bachelor of Science in,
Combined Honours in Environmental Science and Chemistry

at

Dalhousie University

Halifax, Nova Scotia

April 2023

Supervisor: Dr. Craig Brown

©Copyright by Catherine Brennan, 2023

Contents

List of Figures	iii
List of Equations	vi
Abstract	vii
Acknowledgements	viii
Chapter 1- Introduction	1
1.1 Marine Carbon	1
1.1.1 Biological Carbon pump	2
1.1.2 Large-Scale Carbon Stocks.....	3
1.1.3 Habitat Specific Carbon Stocks	4
1.1.4 Organic Carbon Data Collection.....	5
1.2 Seafloor Mapping.....	6
1.2.1 High-Resolution Mapping.....	6
1.2.2 Sediment Classification	7
1.3 Mapping Carbon	8
1.3.1 Backscatter, Grain Size and Carbon	8
1.3.2 Nova Scotian Knowledge Gaps	9
1.4 Summary of Approach	10
Chapter 2 Methods	11
2.1 Regional setting	11
2.2 Seafloor Modeling Approach.....	16
2.3 Geospatial data sets.....	17
2.4 Random Forest Sediment Map.....	20
2.5 In situ sampling.....	22

2.6 Carbon and Organic Matter samples	24
2.7 Grain Size Analysis	25
2.8 Estimation of Total Standing Stock of Organic Carbon	26
3.0 Results	27
3.1 Random Forest	27
3.1.1 Variable selection and performance	27
3.1.2 Model Validation.....	28
3.2 Mapped Substrate Type	29
3.3 Grab samples.....	31
3.4 Relationship between Grain size and Organic Carbon	36
3.5 Organic Carbon in Surficial sediments	38
4.0 Discussion	39
4.1 Comparison between Sediment Map and Previous Studies in the Eastern Shore Islands.	39
4.2 Factors Controlling Organic Carbon.....	40
4.3 Limitations in the study.....	43
4.4 Future Work	44
5.0 Conclusion.....	47
6.0 References	48
7.0 Appendix.....	55
Appendix I: Drop Camera Imagery	55
Appendix II: Sediment classification table	63

List of Figures

- Figure 1.** The geographic extent of the bathymetry and backscatter data in the Eastern Shore Islands. Map created by Catherine Brenan11
- Figure 2.** A multi-resolution surficial geology of the area offshore Clam Harbour to Mooseland along the Eastern Shore of Nova Scotia in 2018. Disregard the letters and red boxes since they accompany other illustrations. Map created by King (2018)12
- Figure 3.** Depth-averaged currents on the ESI. The red arrows are the coastal trapped current (inshore ESI), which is 10 cm/s and 60 m isobath bounded by the coast and the black arrows indicate the offshore ESI, which is moving 20 cm/s and 100 m isobath bounded. Map created by Feng et al. 2022.....13
- Figure 4.** Map of chlorophyll-a concentration (mg/m^3) in the Scotian Shelf and Eastern Shore Island using Sentinel 3 data. Map created by Catherine Brenan14
- Figure 5.** Total suspended matter concentration (mg/m^3) in the Scotian Shelf and Eastern Shore Islands using Sentinel 3 data. Map created by Catherine Brenan.....15
- Figure 6.** Bathymetry data mapped in the Eastern Shore Islands study area. Deeper areas are dark blue and shallower regions are red. Map created by Catherine Brenan and bathymetry processed by Esther Bushuev.18
- Figure 7.** Visualization of Backscatter in the study area. Dark grey features indicate soft sediment, and light grey features are hard substrate. Map created by Catherine Brenan, and backscatter was processed by Esther Bushuev.18
- Figure 8.** Vector Ruggedness Measure mapped in the Eastern Shore Islands study area. Areas of high ruggedness are light pink, whereas smoother areas are black. Map created by Catherine Brenan, and bathymetry processed by Esther Bushuev.....19
- Figure 9.** Slope mapped in the Eastern Shore Islands study area. Areas of an extensive slope are red/orange, whereas flat surface areas are light grey. Map created by Catherine Brenan, and bathymetry processed by Esther Bushuev.19

Figure 10. Drop camera imagery surveys from Fisheries and Oceans Canada combined with carbon sampling from study. Map created by Catherine Brenan and data extracted by Fisheries and Oceans Canada..... 20

Figure 11. Screen shot from video indicating gravel (upper left), cobble/boulder (upper right), bedrock (lower left), mud/sand (lower right). Red 10 cm laser scale visible in middle of images. Overlay on upper left side in yellow shows latitude/longitude of GPS. GMT time and date stamp on upper right in white; local time and date on lower left in white. Camera imagery taken by Department of Oceans and Fisheries. 21

Figure 12. Flow chart outlining the geoprocessing steps of created the sediment classification map. Chart shows data inputs and outputs, processing steps, measurements, and modelling. Created by Catherine Brenan 21

Figure 13. Sample surveys taken in spring 2022. Some sites included samples and drop camera imagery (blue points), while others could only collect drop camera imagery due to the hard substrate (orange points). Map created by Catherine Brenan..... 23

Figure 14. Drop Camera imagery when collecting grab samples to measure OC. Sample 20 consists of granules (top left) whereas sample 21 is finer sediment like sand/mud (Top right). Sample 22 is larger pebbles and cobbles (bottom left) and sample 36 is a mixture of grain and matrix with some pebbles and sand/mud. Scale of each sample is 30 cm. 23

Figure 15. Sediment samples before (left side) and after (right side) loss on ignition method to determine percent organic matter 24

Figure 16. Variable Importance scores. The importance of predictor variables as indicated by the random forest algorithm. The x axis indicates the variables of the final model, the y-axis demonstrates the relative percent importance. Graph created by Catherine Brenan. 27

Figure 17. Confusion Matrix used to determine the sensitivity and accuracy of the map. Chart created by Catherine Brenan 28

Figure 18. The graph indicates the percent accuracy of the most prominent sediment classes in the sediment classification map. The accuracy can help determine the ability of a random forest algorithm to predict the different substrate types. Chart created by Catherine Brenan..... 29

Figure 19. Sediment classification map which was derived using the Forest-Based Classification and Regression tool in ArcGIS Pro. The map was created by Catherine Brenan30

Figure 20. Graph depicting total area (m²) for each sediment type in the substrate classification map. The orange bars indicate the sediment type with the largest total area, which includes mud/sand, gravel/cobble/boulder/bedrock, and gravel/cobble/boulder. Graph created by Catherine Brenan31

Figure 21. Percentage of sediment type for each sample station. Grain size was determined using the Wentworth scale. Graph created by Catherine Brenan33

Figure 22. Quantity of mud (%) and sand (%) found for each sample. Graph created by Catherine Brenan33

Figure 23. OC data that has been displayed in proportional symbols. Each data point is labeled to their correct survey station. Map created by Catherine Brenan34

Figure 24. Backscatter overlaid with organic carbon samples35

Figure 25. Chlorophyll-a concentration which is overlaid with OC measurements. Map created by Catherine Brenan36

Figure 26. Graph depicting a linear regression between OC and percent sand. The grey area represents a 95 percent confidence interval for the slope of the regression line.37

Figure 27. Linear regression graph indicating the relationship between OC and percent mud. The grey area represents a 95 percent confidence interval for the slope of the regression line.37

List of Tables

Table 1. Description of Predictor variables used to model sediment type, including their units and description.....17

Table 2. Results from grab samples including grain size and organic carbon measurements.32

Table 3. Calculations used to determine the total stock of OC in the mud/sand sediment type and the total stock of OC in the entire study site.38

List of Equations

Equation 1. Mean of the squared prediction error equation.....	16
Equation 2. Porosity equation derived from Jenkins & Koenders (2005).....	26
Equation 3. Dry bulk density equation.....	26
Equation 4. Equation used to estimate the standing stock of organic carbon per m ²	26
Equation 5. Accuracy equation.....	28
Equation 6. Sensitivity equation.....	28

Abstract

Coastal sediments contain some of the largest stocks of organic carbon on earth and play a vital role in influencing the carbon cycle. Protecting organic carbon hotspots is essential to mitigating climate change since coastal development and bottom trawling can disturb the seafloor, driving the remineralization of organic carbon into carbon dioxide. Terrestrial carbon stocks are well studied and mapped, but our knowledge of standing stocks of marine sedimentary carbon and the role that it can play in minimizing the effects of climate change are poorly understood. One of the challenges in mapping the seafloor environment is the issue of characterizing spatial heterogeneity of different substrata, which is critical in estimating organic carbon standing stocks in the marine environment.

In this study, we use high-resolution multibeam echosounder (MBES) data from the Eastern Shore Islands off Nova Scotia to predict the distribution of percent organic carbon in surface sediments. We applied benthic habitat mapping approaches, utilizing high-resolution continuous coverage environmental variables (bathymetry, backscatter, ruggedness, and slope) combined with subsea video and sediment grab sample ground truthing to generate thematic maps of sediment types for the area. We then compared that to organic carbon measurements from the sediment samples to estimate organic carbon standing stocks by substrate type. The sediment map had a 60 % mean of the squared prediction error, yet the substrate pattern was like previous substrate maps that were done in the Eastern Shore Islands. We also found that the standing stock of carbon range was 613,536 to 10,915,548 kg/km². Our findings demonstrated that high-resolution sediment classification maps are necessary to improve our understanding of spatial patterns of OC. They can also help identify carbon hotspots, which are essential for seabed management and climate mitigation strategies.

Key words: Organic Carbon, Ocean Sediment, Seafloor Mapping, Marine Carbon Stocks, Seabed Acoustics

Acknowledgements

I would like to first thank my wonderful supervisor Dr. Craig Brown for providing me with continuous guidance throughout this project and allowing me to learn more about the world of seafloor mapping. I am eternally grateful for his drawings and diagrams to help wrap my head around the complexity of seafloor habitat mapping and acoustic remote sensing.

Next, I would like to extend my gratitude to Esther Bushuev for her input when performing analysis on GIS and for taking the time to help me expand on her research on the Scotian shelf. A special thank you to the vessel crew, Larissa Pattison, and Vicki Gazzola, for their support and fieldwork expertise when collecting my sediment samples. Also, the Algar lab provided me with equipment for the field work and was an essential contributor to this research. Dr. Chris Algar provided insight into chemical oceanography and how to effectively measure organic carbon on the seafloor. Maria Armstrong taught me how to collect sediment samples and perform organic matter analysis. Furthermore, I extend my thanks to Adam White for his tremendous help in collecting grain size measurements at the Bedford Institute of Oceanography. I would also like to thank Dr. Tarah Wright for her feedback and guidance on writing and developing an effective research proposal. Lastly, I would like to thank the Department of Earth and Environmental Science for awarding me the Michael J. Keen award, which supported my fieldwork over the summer.

Chapter 1- Introduction

1.1 Marine Carbon

Climate change is the most pressing issue of our time, and one way to mitigate climate change is to protect ecosystems that undergo carbon sequestration. In the carbon cycle, carbon travels from different reservoirs, such as oceans, organisms, minerals, and the atmosphere, through numerous mechanisms (Nellemann et al., 2009). There are also multiple forms of carbon, including inorganic carbon, which is bound in minerals, and organic carbon, which is derived in nature from living organisms.

Within the global carbon cycle, 93% of carbon is stored and cycled in our oceans, making it an essential energy source for marine biodiversity (Nellemann et al., 2009). Carbon stored and captured in ocean ecosystems is known as blue carbon, and the global ocean can store disproportionate amounts of organic carbon compared to terrestrial carbon stocks (Hilmi et al., 2021). The Intergovernmental Panel on Climate Change (IPCC) defines blue carbon as: “All biologically driven carbon fluxes and storage in marine systems that are amenable to management.” (Hilmi et al., 2021). Blue carbon is often associated with vegetation in coastal zones, such as tidal marshes, mangroves, and seagrasses (Fourqurean et al., 2012; Sanders et al., 2016). Phytoplankton productivity at the surface of the oceans has also been at the center of blue carbon research estimating marine carbon through aerial imagery (Chase et al., 2022). There is still some debate over whether the blue carbon concept should include other coastal and non-coastal ecosystems, such as marine sediments (Hilmi et al., 2021).

Organic carbon (OC) in marine sediments is a critical component of the global carbon cycle and is linked to Earth’s climate (Hilmi et al., 2021). In recently deposited marine sediment, the oxidation of OC controls the fluxes of oxygen and nutrients across the sediment-water interface (SWI), impacting primary productivity in the water (LaRowe et al., 2020). Also, the small amount

of photosynthetically produced OC that escapes degradation and is buried in the sediment can help modulate atmospheric CO₂ over geological time scales and enable oxygen to accumulate in the atmosphere (LaRowe et al., 2020). It is essential to explore marine sedimentary carbon, especially in coastal regions when the seafloor is heterogenous, comprising a patchwork of the substrate. Different substrate types can bury and remove OC from the active carbon cycle, ultimately leading to long-term carbon sequestration (Hunt et al., 2021). For instance, fine sediments can store more OC than coarser sediment since mud has low oxygen conditions, which reduces the rate of microbial decomposition of OC efficiently compared to microbial decomposition of OC in well-oxygenated sediment (Bianchi et al., 2023). Understanding the spatial distribution of OC in marine sediments can therefore help us determine carbon hotspots and manage activities that cause the resuspension of buried OC.

1.1.1 Biological Carbon pump

Before carbon can reach the seafloor from the atmosphere, it needs to pass through the water column through the process known as the biological carbon pump. The biological carbon pump is the mechanism that exports carbon-containing compounds via biological processes from the surface to the deep ocean (Sarmiento & Gruber, 2006). During primary production, phytoplankton converts nutrients and dissolved inorganic carbon (DIC) into particulate organic carbon (POC), which lowers the partial pressure of carbon dioxide (CO₂) and allows the ocean to absorb CO₂ from the atmosphere (Claustre et al., 2021). Organisms then consume portions of POC within the ocean's interior, and the excess fraction, known as marine snow, is the organic material that falls from the upper water column to the seafloor. Before undergoing sediment deposition, the POC must first traverse the "benthic transition zone" (Turnewitsch et al., 2017). The benthic transition zone is the lower part of the water column in which the seafloor has a direct influence on biogeochemical activity. This region has been argued to have an increase in residence time of particulate carbon, which allows more time for a microbially driven breakdown of organic matter before final deposition into the underlying sediments.

(Turnewitsch et al., 2017). Over time the OC-rich deposits start to accumulate, allowing the OC to transition from the fast-cycling surficial reservoirs (i.e., the ocean, atmosphere, biosphere, upper sediment) into the slow carbon cycle (i.e. the geological reservoirs) (Bradley et al., 2022). The slow carbon cycle governs climate change on a timescale of millions of years, while the fast carbon cycle regulates decades to millennia (Bradley et al., 2022). The sedimentation of POC is therefore essential to transferring CO₂ from the atmosphere to the seabed, mitigating increases in atmospheric CO₂ associated with climate change (Diesing et al., 2017). Many studies have investigated the biological carbon pump and found that there is still limited knowledge concerning benthic-pelagic fluxes of carbon and how climate change will alter carbon storage efficiency (Snelgrove et al., 2018).

1.1.2 Large-Scale Carbon Stocks

To understand how OC storage will change with climate change and human pressure conditions, it is first necessary to quantify the carbon stock. Studies that undergo large-scale carbon stocks can have oversimplification and inconsistency in carbon averaging. Snelgrove et al. (2018) formed a carbon budget for the Northwest European continental shelf by examining pelagic, coastal, and benthic carbon stocks. They determined that benthic carbon stocks had an increased uncertainty due to the high spatial variability in terms of substrata and an immense range in the per-unit area carbon storage in the different sediment types. In addition, they noted that in most carbon studies, biogeochemists, despite emphasizing substantial gradients in the sediment column, tend to ‘average’ seafloor rates and processes spatially. Other studies, like Atwood et al. (2020), quantified global marine sedimentary C stocks at a 1- km resolution using C data from published papers. This search resulted in C data for 15,0004 cores. However, the sediment C data was not uniform with a large data gap in the Southern Ocean. Also, Atwood et al. (2020) suggested that the data from the published papers they studied could have had a bias toward more organic-rich or organic-poor sediments. Furthermore, the inability to easily collect POC concentrations in coarse-grained sediments often leads studies to assume the concentration is zero in these substrate types (Burrows et al., 2014). Generally, it is difficult

to sample a coarser sediment matrix, and these sediment types are often under-represented in sedimentary carbon studies (Hunt et al., 2021). Another important consideration with broad-scale carbon stocks is that most have occurred in fjords (Smeaton et al., 2019; 2021; Hunt et al., 2020). Fjords have been established as long-term stores of both OC and inorganic carbon (IC). The quantity of OC is often incorrectly estimated due to the complex spatial heterogeneity of fjord sediments (Smeaton & Austin, 2019). Studies done in only fjords suggest that there is limited knowledge on the heterogeneous seabed in exposed coastal environments.

These studies highlight the challenges of determining carbon stocks on a broad spatial scale. The application of models to broad-global scale projections often requires simplification and averaging, which can eliminate the complexity on the seafloor. Also, due to a lack of mapping data, physical OC measurements when scaled up to standing stocks would assume a similar bottom type throughout an area. This emphasizes that we have a poor understanding of OC in heterogeneous sediment due to a lack of accurate high-resolution seafloor mapping of surficial sediment.

1.1.3 Habitat Specific Carbon Stocks

Most studies of carbon stocks examine specific habitat types leading to a bias in data collection. Recently, carbon stock studies have focused on vegetated coastal ecosystems, such as mangroves (Sanders et al., 2016) and seagrasses (Fourqurean et al., 2012). Araújo et al. (2016) mapped kelp forest distribution in Svalbard, Norway, the Baltic Sea, France, the UK, and the Mediterranean Sea. Large-scale spatial trends of kelp forests were assessed due to their ability to undergo natural carbon sequestration. Another study done by Arias-Ortiz et al. (2018) used field studies and satellite imagery to quantify the amount of total seagrass area lost due to heatwaves and used a mixing model to determine the average contribution of seagrass to the sediment C stocks in Shark Bay Western Australia. Macro-tidal salt marshes have also been examined since they are net carbon sinks with the potential for long-term carbon storage (Artigas et al., 2015).

In summary, many studies have examined vegetated coastal and intertidal habitats (Seagrass, kelp forests and salt marshes) since they are often accessible and easily measurable. Marine and coastal sediments, on the other hand, have heterogeneous substrates, which can be challenging to sample due to the poor efficiency or inability of benthic samplers (e.g., cores and grabs) for measuring carbon in coarse substrates such as consolidated gravels, cobbles, boulders, and bedrock. Offshore areas are also not easily accessible and can be more costly to retrieve samples than intertidal habitats. However, it is still imperative to examine marine and coastal sediments because they cover a wider area than vegetated coastal and intertidal habitats, allowing them to provide a greater area for carbon storage.

1.1.4 Organic Carbon Data Collection

There have been various approaches to collecting OC measurements in carbon stock studies. A study done by Smeaton et al. (2021) had no spatial component and compiled fifteen sediment cores between 2016 and 2019. Each core was sliced and freeze-dried to determine bulk elemental OC composition. They also collected wet bulk density values, stable isotopes ($\delta^{13}\text{C}_{\text{Org}}$ and $\delta^{15}\text{N}$) and radiometric dating. Radiocarbon ages were acquired from shells found in the sediment cores to estimate longer-term (100s–1000s of years) sedimentation and accumulation rates. In another study, Diesing et al. (2017) used 1,111 measurements of the concentration of POC in the grain size fraction <2 mm from seafloor sediment samples collected between 1996 and 2015 to create a spatial model of POC on the seafloor. Sediments were freeze-dried and formed into a powder, and IC was removed via sulphurous acid digestion. Hunt et al. (2020) examined OC spatially, using 28 grab samples, and homogenized the bulk sediment to be freeze-dried. Then they measured sedimentary OC, total carbon, and total nitrogen content using an elemental analyzer. The coarse-grained sediments that they collected were not measured for elemental analysis.

Each of the above studies adopted a different approach on what to collect when examining OC on the seafloor. Studies that lacked a spatial component (Smeaton et al. 2017; 2021) usually measured multiple variables associated with carbon, such as radiocarbon dating and stable isotopes. The studies that attempted to map carbon (Hunt et al. 2020; Diesing et al. 2017), only considered one or two measurements, such as the concentration of POC and total nitrogen. This suggests that spatially mapping OC is still a new approach and lacks complex measurements of carbon, which is critical to comprehend the elaborate processes of carbon on the seafloor.

1.2 Seafloor Mapping

1.2.1 High-Resolution Mapping

There is a lack of high-resolution seafloor mapping data available for the global ocean, with only 18% of the seafloor mapped using echo sounders at a resolution of about 1 km (Mayer et al., 2018). However, recent advancements in multibeam-echosounder surveys (MBES) have led to the ability to create spatially continuous high-resolution maps of the ocean floor (Brown et al., 2011; Buhl-Mortensen et al., 2021). In the past, MBES has been very expensive, but recent improvements with accessing the technology allow us to sufficiently map the spatial complexity on the seafloor (Wöflfl et al., 2019). MBES collects bathymetry and backscatter which provides information about the composition of the seafloor, such as the morphology, hardness, sediment characteristics, and sediment grain size (Brown et al. 2011). Bathymetry is the delay between the emission of the pulse and receipt of the returned signal, which provides a measurement of the depth of the seafloor (Smeaton & Austin, 2019), while backscatter is determined by the strength of the returned signal indicating the reflectivity of the seafloor, and is often used as a proxy for substrate (Smeaton & Austin, 2019).

1.2.2 Sediment Classification

Traditionally, seafloor sediment mapping has relied heavily on expert practitioners and high amounts of ground truthing to classify sediment types (Eleftheriou & McIntyre, 2005; Gregory & Anderson, 1997). Yet grab sampling is often time-consuming, expensive and can result in low-resolution maps due to the difficulty of acquiring accurate boundaries between different sediments.

Recently, the procedure for deriving seafloor sediment maps has shifted, and more studies now include the use of MBES data combined with amounts of in situ seafloor sampling data (ground truthing and visual information) to create continuous thematic maps (Buhl-Mortensen et al., 2021). A thematic map is a map that demonstrates the spatial distribution of one or more specific data themes for a selected geographic area (Statistics Canada, 2018).

Ground truthing can be in various forms, but typically physical sediment samples or optical imagery can be used to verify seafloor substrata. A complete coverage of the seafloor is predicted by combining the ground truthing data, which is a small proportion of the study area and the MBES data (Brown et al. 2011). The MBES data can act as a proxy to estimate the areas that did not undergo direct in situ sampling (Brown et al., 2011).

MBES bathymetry is a crucial variable for sediment maps since it provides information about the seafloor morphology, including slope, ruggedness, and curvature. These terrain metrics are essential for deriving and segmenting seafloor geology (Proudfoot et al., 2020). MBES backscatter can provide a proxy measure of sediment type, with strong backscatter signals typically representing hard, consolidated substrates while low backscatter corresponds to soft, unconsolidated substrates (Proudfoot et al., 2020).

In addition, Geographic Information Systems (GIS) and machine learning approaches have allowed for increased accuracy in using MBES data and other predictor variables to form reliable seabed sediment maps (Galvez et al., 2022; Wölfl et al., 2019). These automated seafloor mapping approaches can be less time-consuming and are often more reproducible and robust than manual classification (Brown et al., 2011; Misiuk et al., 2019). Despite the progress made in recent years, seafloor sediment classification and monitoring using reproducible and automated methods is still in its infancy (Janowski et al., 2020). More sediment mapping studies must be performed to determine the ideal machine learning approach and to predict sediment classes in complex heterogeneous seafloor.

1.3 Mapping Carbon

1.3.1 Backscatter, Grain Size and Carbon

Recent carbon studies have suggested a relationship between sediment grain size, seafloor bathymetry/backscatter data sets, and OC. Diesing et al. (2017) created a random forest model of POC using predictor variables, such as distance to shoreline, mud content, peak wave orbital velocity, gravel content and annual average bottom temperature. After deriving a POC map, they determined that mud contents in surface sediments are the most significant variable to POC. Yet, they also noted that sand and gravel contributed the most to POC stock due to the widespread occurrence of the sediment type. This connection between sediment grain size and OC is well known but has never been scaled spatially due to a lack of accurate heterogeneous substrate maps. Similarly, Hunt et al. (2020) used MBES backscatter as a proxy for grain size to predict OC and determined that acoustic backscatter improves the accuracy of the spatial OC model by 14%. The study indicated that the backscatter survey reliably uncovers a heterogeneous seabed and that OC correlates strongly with the MBES backscatter signal as a function of sediment composition (Hunt et al., 2020). Furthermore, studies examining sediment characteristics and carbon storage in seagrass meadows found that when performing a regression analysis, there was a significant positive correlation between the percent mud and sediment C stocks (Lima et al., 2020; Leduc et al., 2023). Lima et al. (2020) also ran a partial

least squares regression model, and the most important predictor variables responsible for the variation in sediment C stock included percent mud and mean grain size. In all, there is evidence to suggest that there is an empirical relationship between OC and sediment grain size and acoustic backscatter correlation with grain size. Yet, only a few studies have been able to explore that relationship.

1.3.2 Nova Scotian Knowledge Gaps

Carbon mapping is still a new area of study and has been explored in only a few locations globally. Some studies of carbon stocks have been researched in the North American Coastal region, but without spatially explicit estimates (Fennel et al., 2019; Najjar et al., 2018). Others have occurred in the United Kingdom and a focus on North-West European continental shelf sediments (Diesing et al., 2017, 2021; Hunt et al., 2020; Hunt et al., 2021; Legge et al., 2020; Smeaton et al., 2021; Smeaton & Austin, 2019). In all, there has been no examination of the use of seafloor mapping techniques to determine standing stocks of OC on the seabed in the Scotian Shelf, and future studies should be done in this area to eliminate the knowledge gap.

1.4 Summary of Approach

This research aims to answer the following questions:

- Can we predict the seafloor substrate type in the benthic environment using multibeam echosounder surveys in the offshore Eastern Shore Islands, Atlantic Canada?
- Can we use high-resolution substrate classification maps to estimate the standing stock of organic carbon in the sediments of the offshore Eastern Shore Islands, Atlantic Canada?

Our study will use high-resolution MBES survey data combined with drop camera imagery of the sediment type to model the substrate classes. We will then use the sediment map, sediment grain size and total organic carbon (TOC) measurements to derive a total standing stock of OC. The study focuses on the Eastern Shore Islands, an Area of Interest (AOI) off the east coast of Nova Scotia (Figure 1). The site is in Canada, which is different from previous studies that have predominantly taken place in the United Kingdom (Hunt et al., 2020; Smeaton & Austin, 2019). Also, deriving total OC using a sediment map could provide insight on the value of high-resolution mapping in OC studies. Lastly, it can help re-examine the importance of this marine protected area in providing climate regulation services and can be a tool for finding future carbon hotspots across the Scotian Shelf.

Chapter 2 Methods

2.1 Regional setting

The study site is located within the Eastern Shore Islands (ESI), an area of interest (AOI) for conservation objectives on the eastern shore of Nova Scotia, Canada (Figure 1). The site stretches from Clam Bay near Jeddore Harbor to Barren Island near Liscomb Point and extends approximately 25 km from the mainland in the Scotian Shelf region with a depth of approximate 30 m near the coast and 100 m offshore (Jeffery et al., 2020).

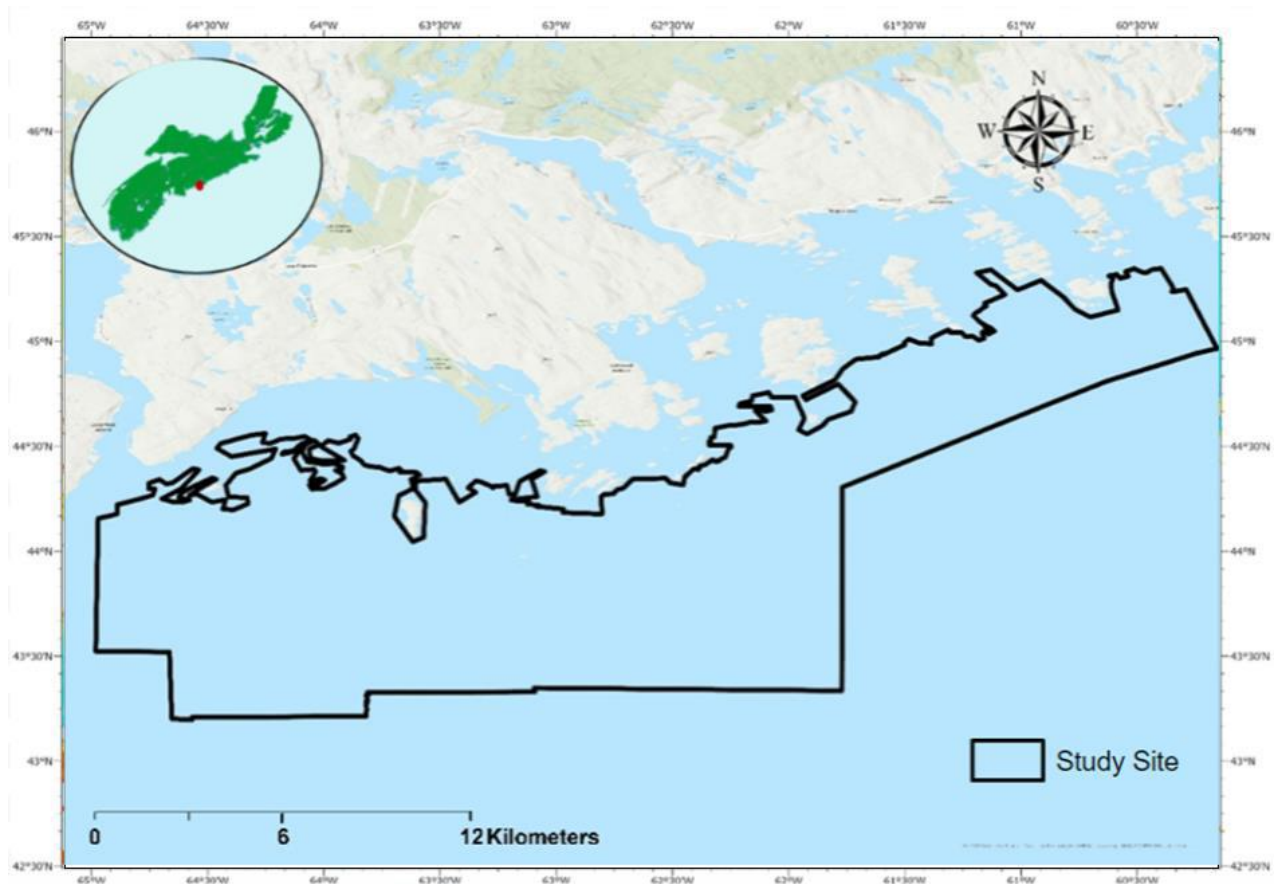


Figure 1. The geographic extent of the bathymetry and backscatter data in the Eastern Shore Islands. Map created by Catherine Brenan.

The seabed character of the ESI is primarily bedrock since it continues from the geomorphology of the land (King, 2018). The bedrock topography heavily influences the type and distribution of the surficial deposits. The glacial imprint is substantial in the area, depositing a sequence of till and glaciomarine mud, which lie directly on the bedrock (King, 2018). There is also a thin layer of wave-modified sand and gravel. Marine mud is the latest significant depositional unit due to estuarine, or lacustrine and coastal deposits (Jeffery et al., 2020). The ESI surficial geology has high spatial variability and is heterogeneous, with bedrock overlaid by mud, sand, gravel, cobble, and boulder substrates (Figure 2).

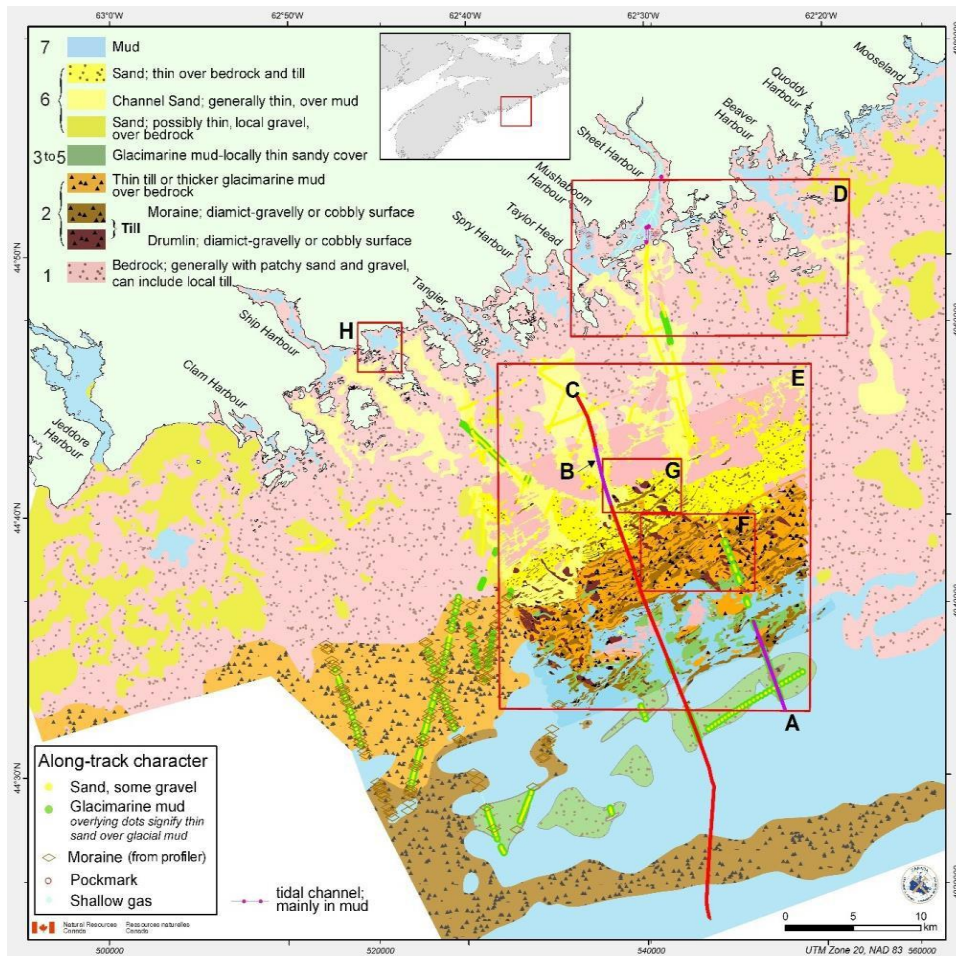


Figure 2. A surficial geology of the area offshore Clam Harbour to Mooseland along the Eastern Shore of Nova Scotia in 2018. Disregard the letters and red boxes since they accompany other illustrations. Map created by King (2018)

Ocean surface and bottom temperatures in the ESI are colder than the Scotian shelf south of Halifax (Jeffery et al., 2020). The ocean current runs mostly southwestwards on the ESI, with some fluctuation around the coast (Feng et al., 2022) (Figure 3). The combination of upwellings, currents, and wind allows for the mixing of nutrients, acting as an essential component of the marine food web in the region (Jeffery et al., 2020).

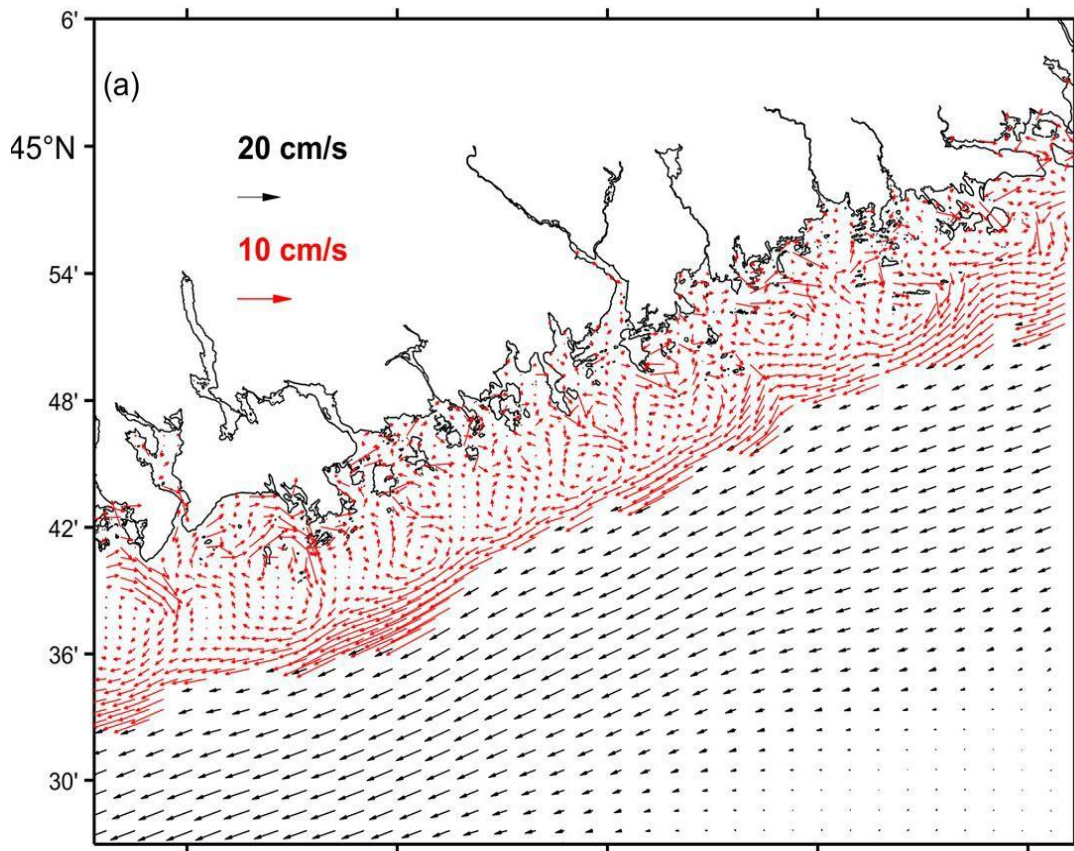


Figure 3. Depth-averaged currents on the ESI over a one-year time period. The red arrows are the coastal trapped current (inshore ESI), which is 10 cm/s and 60 m isobath bounded by the coast, and the black arrows indicate the offshore ESI, which is moving 20 cm/s and 100 m isobath bounded. Map created by Feng et al. 2022.

Nutrients (nitrogen, phosphorus, and silicon) are derived from coastal runoff and are depleted in the spring due to phytoplankton blooms and replenished in the fall when upwelling is predominant (Jeffery et al., 2020). This can be represented in Figure 4 & 5 since there are larger quantities of chlorophyll-a and total suspended matter concentration near the coast in the ESI.

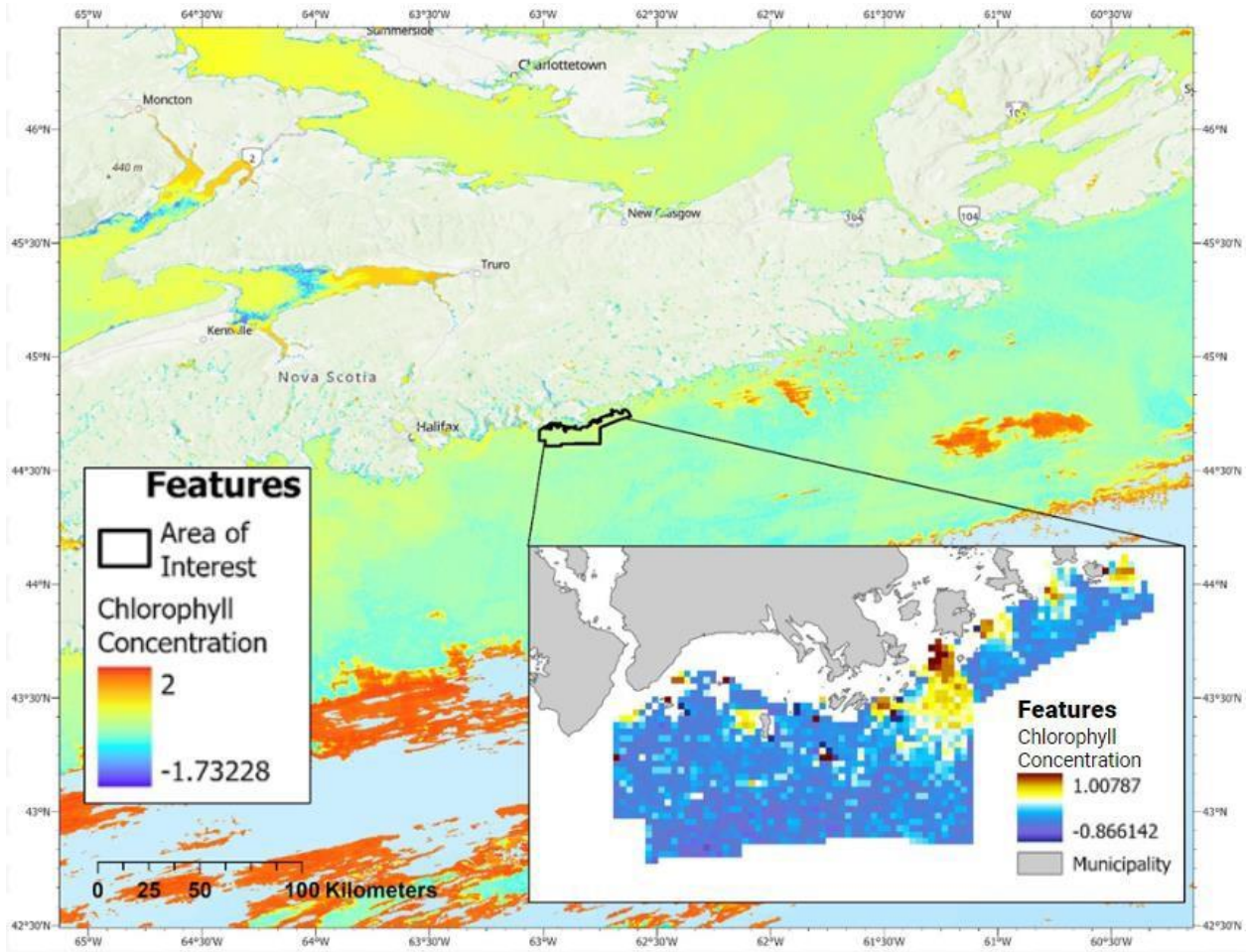


Figure 4. Map of chlorophyll-a concentration (mg/m^3) in the Scotian Shelf and Eastern Shore Island using Sentinel 3 data. Map created by Catherine Brenan.

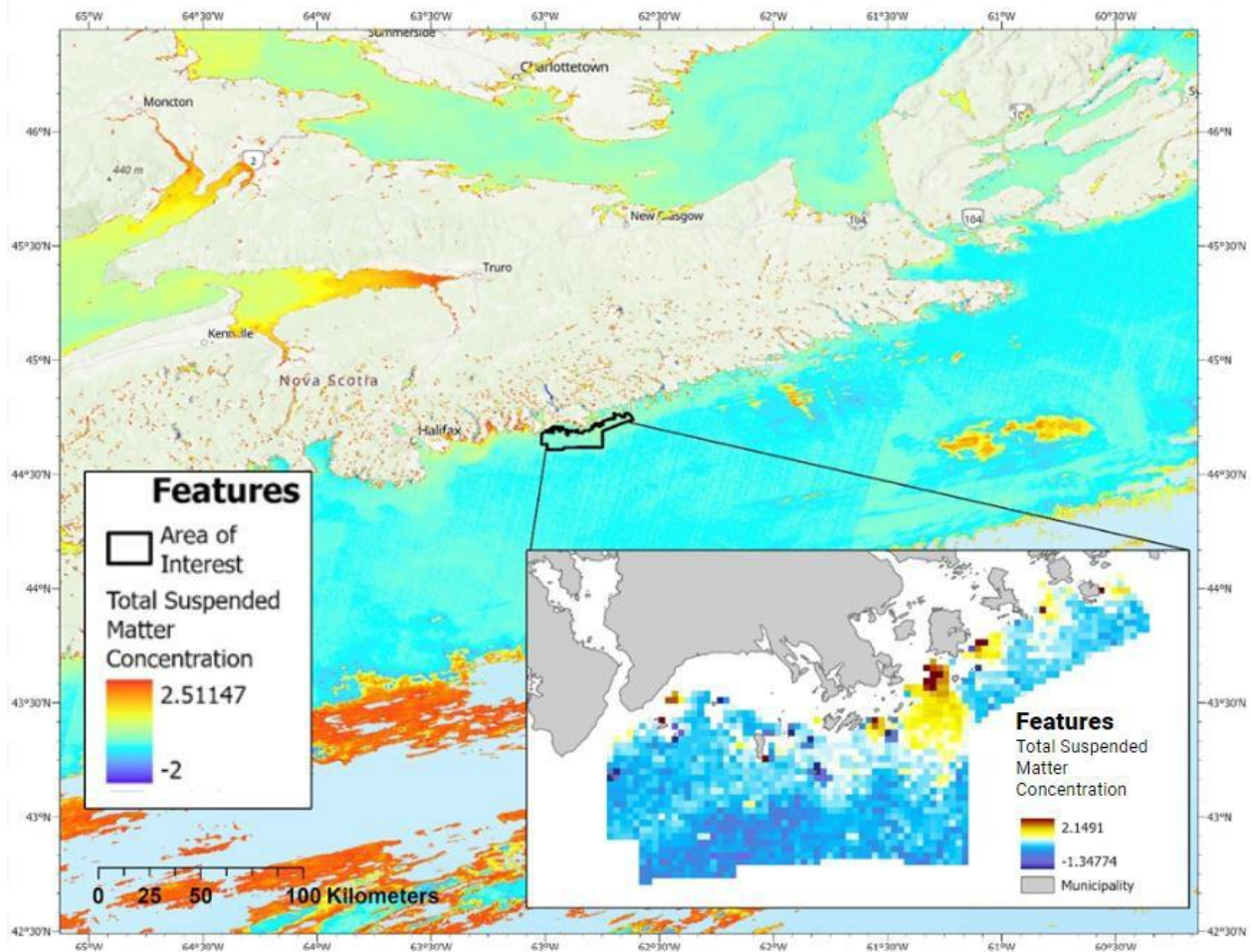


Figure 5. Total suspended matter concentration (mg/m^3) in the Scotian Shelf and Eastern Shore Islands using Sentinel 3 data. Map created by Catherine Brenan.

Major anthropocentric activities in this area include lobster fishing, recreational fishing and boating, but the human impact is generally low due to low population density and coastal development compared to Halifax and St Margaret's Bay (Jeffery et al., 2020).

2.2 Seafloor Modeling Approach

The machine learning approach, random forest (RF), has been used in previous carbon map studies due to its high predictive accuracy, ability to handle many predictor variables and unbiased approach (Diesing et al., 2017). First, the user trains the algorithm to determine the relationship between the ground-truthing data and the predictor variables. Then the algorithm tests a random subset of variables at each split in each tree to decrease bias. Also, RF can tell you which predictor variables correlate to your ground-truthing data. This removes the predictor variables with low correlation to improve accuracy. Furthermore, it can reduce redundancy without losing information content and increase the interpretability of the model (Diesing et al., 2017). Once all the unnecessary predictor variables have been removed, the data is interpolated to your desired area to create a spatially continuous map. In the study, 100 trees were examined, which is the default setting.

Random forest carries out cross-validation using out-of-bag observation. These are defined as 10% of the training features that are held back in the training model (Diesing et al., 2017). After the model has been trained, the held-back training features are run, and a mean of the squared prediction error is calculated in the equation (1) below:

$$MSE_{\hat{y}} = \frac{1}{n} \sum_{i=1}^n (y_i - \hat{y}_i)^2 \quad (1)$$

where y are observed and \hat{y} are predicted values.

2.3 Geospatial data sets

A range of geospatial data sets were selected to be used as predictor environmental variables based on their availability and expected relevance to determining substrate type. The predictor variables were at 2 m by 2m pixel resolution and included bathymetry, backscatter, vector ruggedness measure (VRM) and slope (Table 1) (Figure 6-9). VRM and slope were derived from bathymetry using the benthic terrain modeller tool in ArcGIS Pro.

Table 1. Description of predictor variables used to model sediment type, including their units and description.

Environmental variables	Description	Horizontal resolution	Units
Bathymetry	Depth	2m	meter
Backscatter	Measure of intensity of acoustic signal from MBES and indicator of bottom hardness	2m	intensity
Slope	Measures maximum change in elevation (steepness)	2m	degrees
Vector Ruggedness Measure	Measures terrain ruggedness of grid cells within a neighborhood	2m	metres

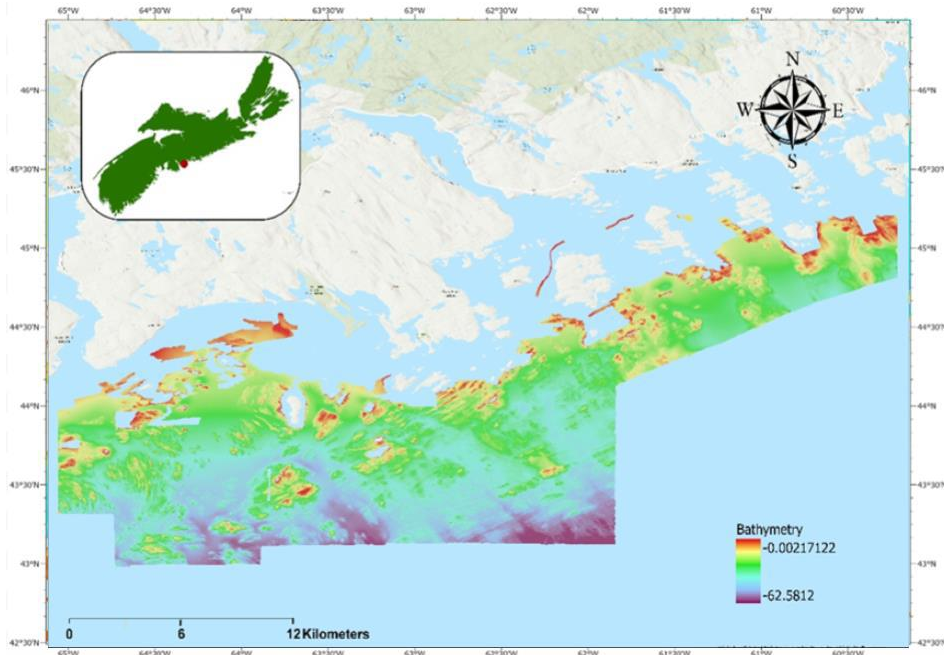


Figure 6. Bathymetry data mapped in the Eastern Shore Islands study area. Deeper areas are dark purple and shallower regions are red. Map created by Catherine Brenan and bathymetry processed by Esther Bushuev.

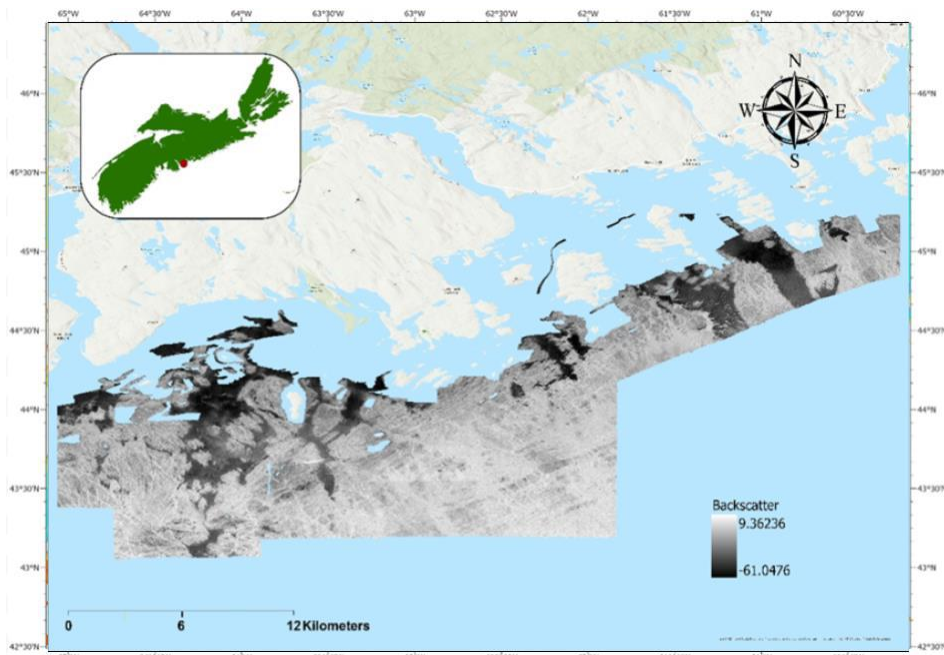


Figure 7. Visualization of backscatter in the study area. Darker colours indicate soft sediment, and light grey features are hard substrate. Map created by Catherine Brenan, and backscatter was processed by Esther Bushuev.

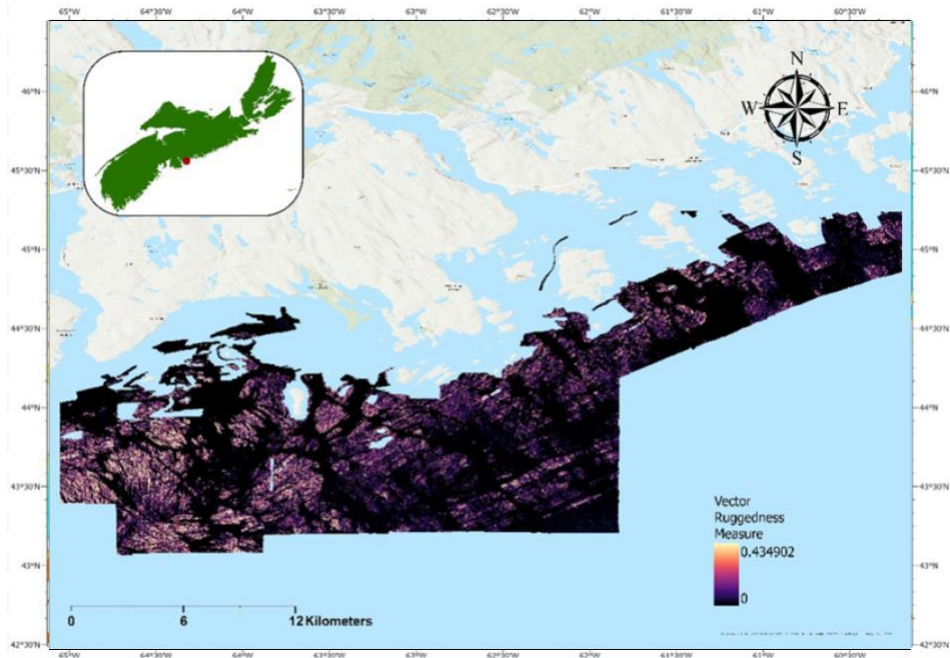


Figure 8. Vector Ruggedness Measure (VRM) mapped in the Eastern Shore Islands study area. Areas of high ruggedness are light pink, whereas smoother areas are black. Map created by Catherine Brennan, and bathymetry processed by Esther Bushuev

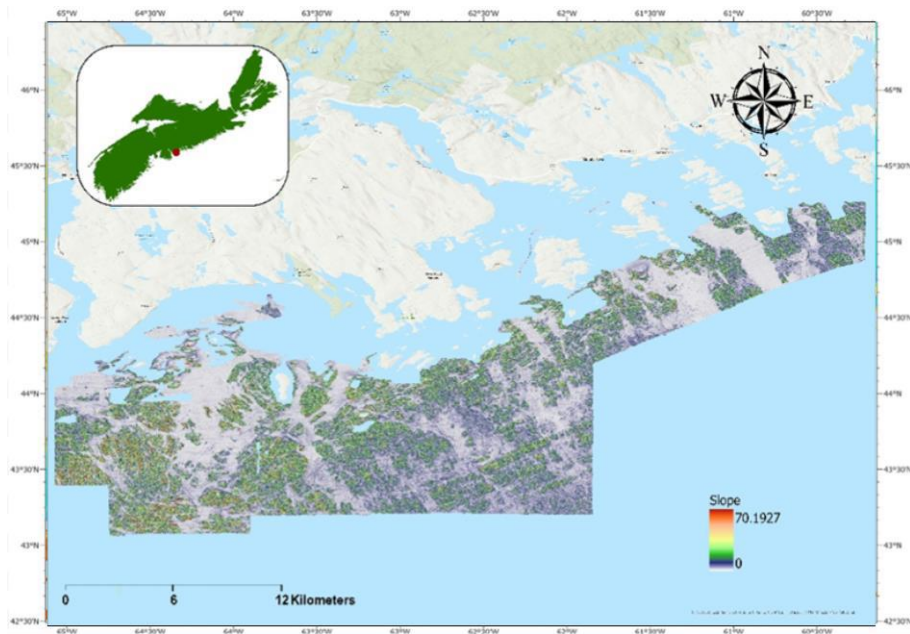


Figure 9. Slope mapped in the Eastern Shore Islands study area. Areas of an extensive slope are red/orange, whereas flat surface areas are light grey. Map created by Catherine Brennan, and bathymetry processed by Esther Bushuev.

2.4 Random Forest Sediment Map

A total of 174 drop camera stations were conducted over 13 days during September and October by DFO in 2017 (Jeffery et al., 2020) (Figure 10). From each video station, a presence (1) and absence (0) of different sediment classifications were obtained. The data included four sediment types: mud/sand, gravel, cobble/boulder, and bedrock (Jeffery et al., 2020) (Figure 11). The camera imagery collected from this study (Section 2.5) was then incorporated with imagery conducted by DFO. The sediment type that was present at each survey location was combined manually from a single class to a merged substrate class (see appendix II). Then, the dataset was put into ArcGIS Pro to combine with the predictor variables, generating a predicted substrate map for the area (Figure 12). The substrate classification map was created in ArcGIS Pro using the random forest classification and regression tool.

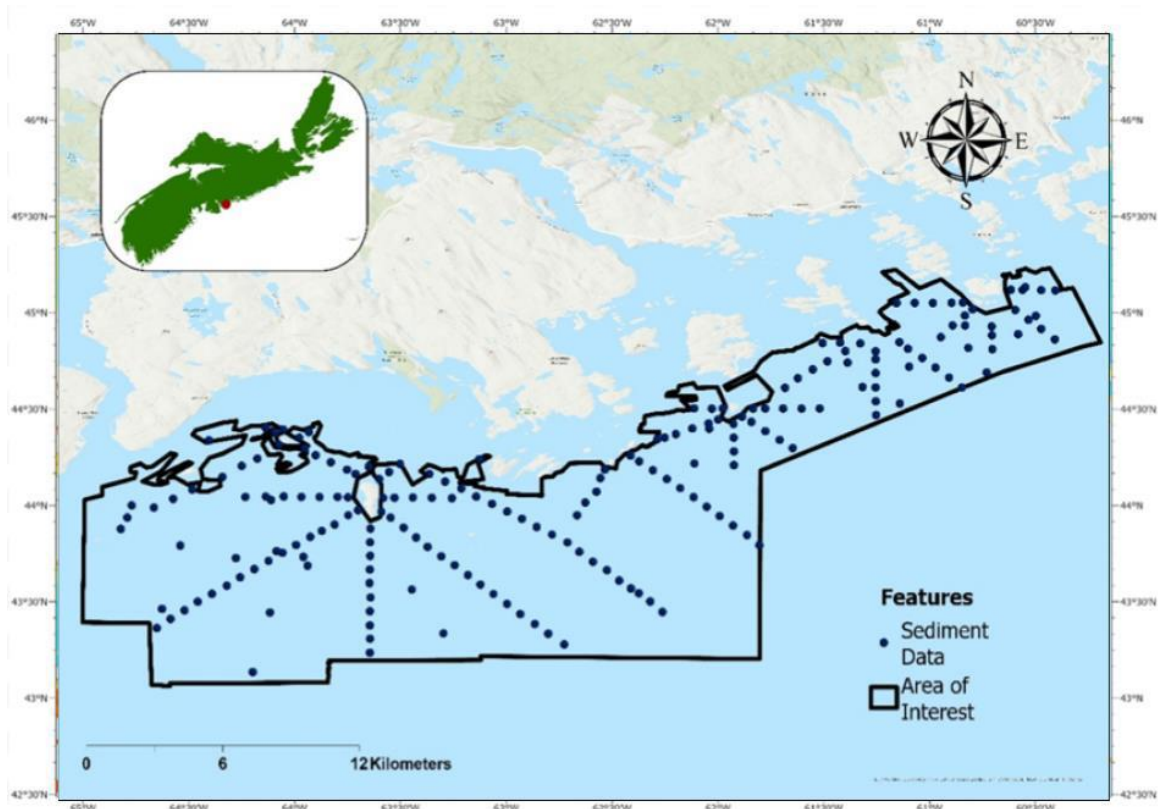


Figure 10. Drop camera imagery surveys from Fisheries and Oceans Canada combined with carbon sampling from study. Map created by Catherine Brenan and data extracted by Fisheries and Oceans Canada.

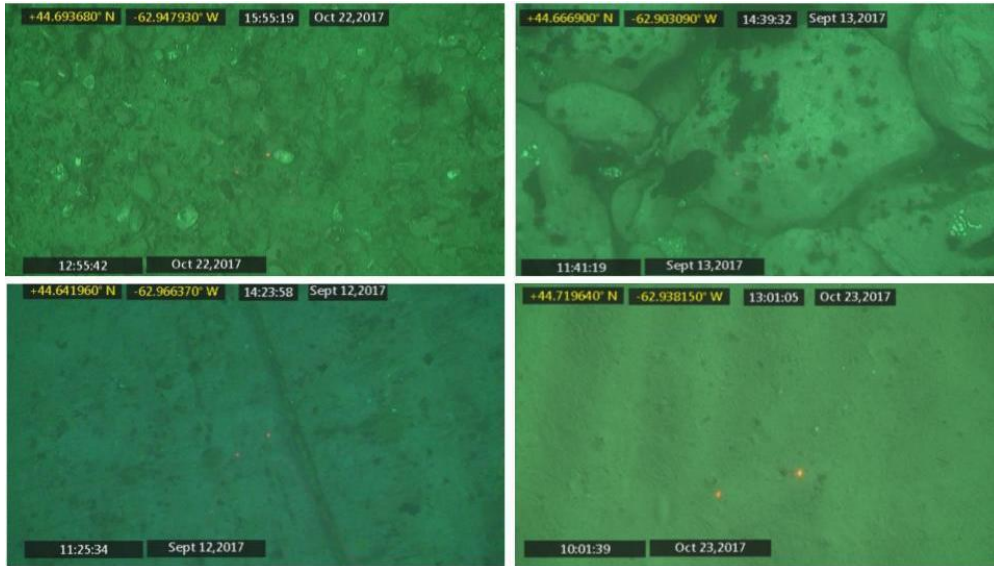


Figure 11. Screen shot from video indicating gravel (upper left), cobble/boulder (upper right), bedrock (lower left), mud/sand (lower right). Red 10 cm laser scale visible in middle of images. Overlay on upper left side in yellow shows latitude/longitude of GPS. GMT time and date stamp on upper right in white; local time and date on lower left in white. Camera imagery taken by Department of Oceans and Fisheries.

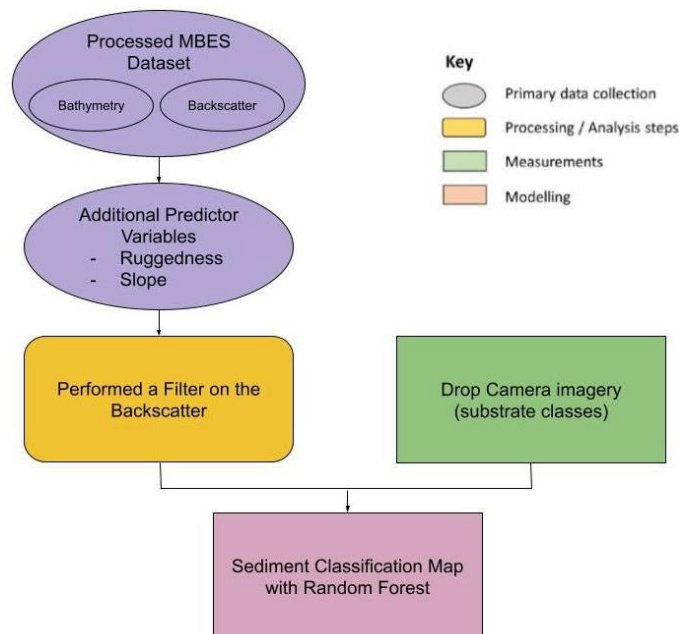


Figure 12. Flow chart outlining the geoprocessing steps of created the sediment classification map. Chart shows data inputs and outputs, processing steps, measurements, and modelling.

Created by Catherine Brennan

2.5 In situ sampling

Sample surveys for OC and grain size were conducted from May 9th to May 27th, 2022. A stratified random sampling technique was used based on the backscatter data (Figure 13). Acoustic backscatter was used to select sampling locations since it is a good predictor of sediment grain size and is common in substrate classification routines (Hunt et al., 2020). A Van Veen grabs sampler fitted with a GoPro camera was operated to collect sediment samples and drop camera imagery at each sample site, with the grab penetrating up to 10 cm depth into the substrate (Figure 14). A GPS position was collected from the research vessel at the point of contact on the seabed at each grab station. Some grab deployments did not receive a sample since the substrate was too coarse (the grab was unable to sample bedrock, boulders, or cobbles). Generally, it is difficult to sample a coarser sediment matrix successfully, and these sediment types are often under-represented in sedimentary C studies (Hunt et al., 2020). After thoroughly mixing the sediment in the Van Veen grab, subsamples of sediment were taken from the grabs and placed in a 32 oz plastic container. These were stored in a cooler during the day and put into a freezer in the evening. It is important to note that the container was not directly frozen after being sampled, so some biological activity could have occurred, which would slightly alter the OC quantity.

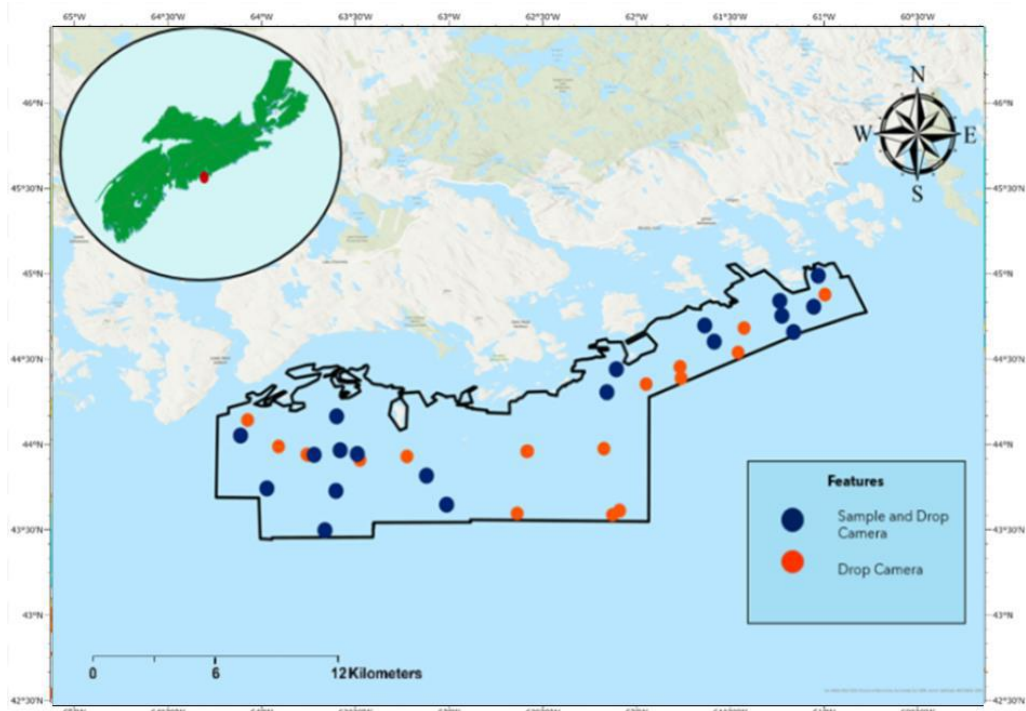


Figure 13. Sample surveys taken in spring 2022. Some sites included samples and drop camera imagery (blue points), while others could only collect drop camera imagery due to the hard substrate (orange points). Map created by Catherine Brennan.

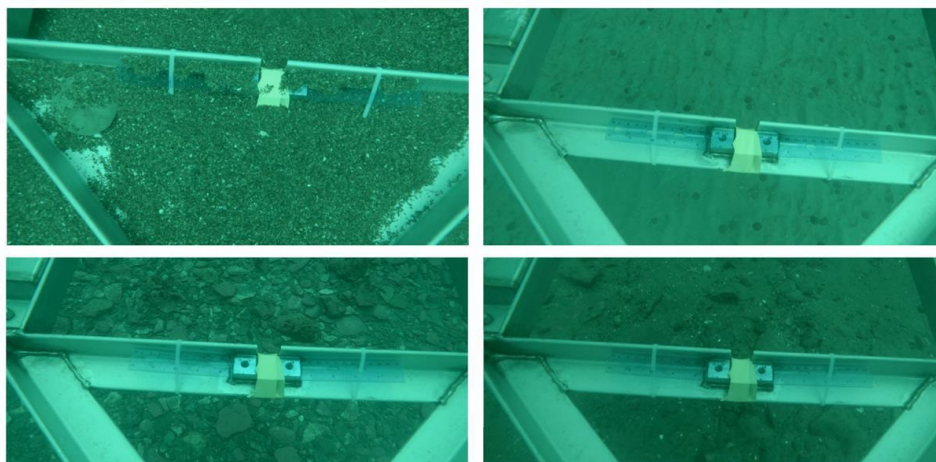


Figure 14. Drop Camera imagery when collecting grab samples to measure OC. Sample 20 consists of granules (top left) whereas sample 21 is finer sediment like sand/mud (Top right). Sample 22 is larger pebbles and cobbles (bottom left) and sample 36 is a mixture of grain and matrix with some pebbles and sand/mud. The scale in each photo is indicated with the 30 cm ruler.

2.6 Carbon and Organic Matter samples

Organic matter (OM) was quantified using a loss-on ignition method (Howard & Howard, 1990). Each sample was dried in an oven overnight to remove any excess water at 50 °C. The sediment was weighed in a 50 mL glass beaker to determine the initial mass (approximately 20 g) and baked in the furnace at 400 °C for 8 hours (Figure 15), with the difference in weight representing the quantity of organic matter. Organic matter is primarily made up of OC (58%), with the remaining mass consisting of water and other nutrients (Bianchi et al., 2008). This indicates that OM can be used to provide insight into the amount of carbon in a sample.

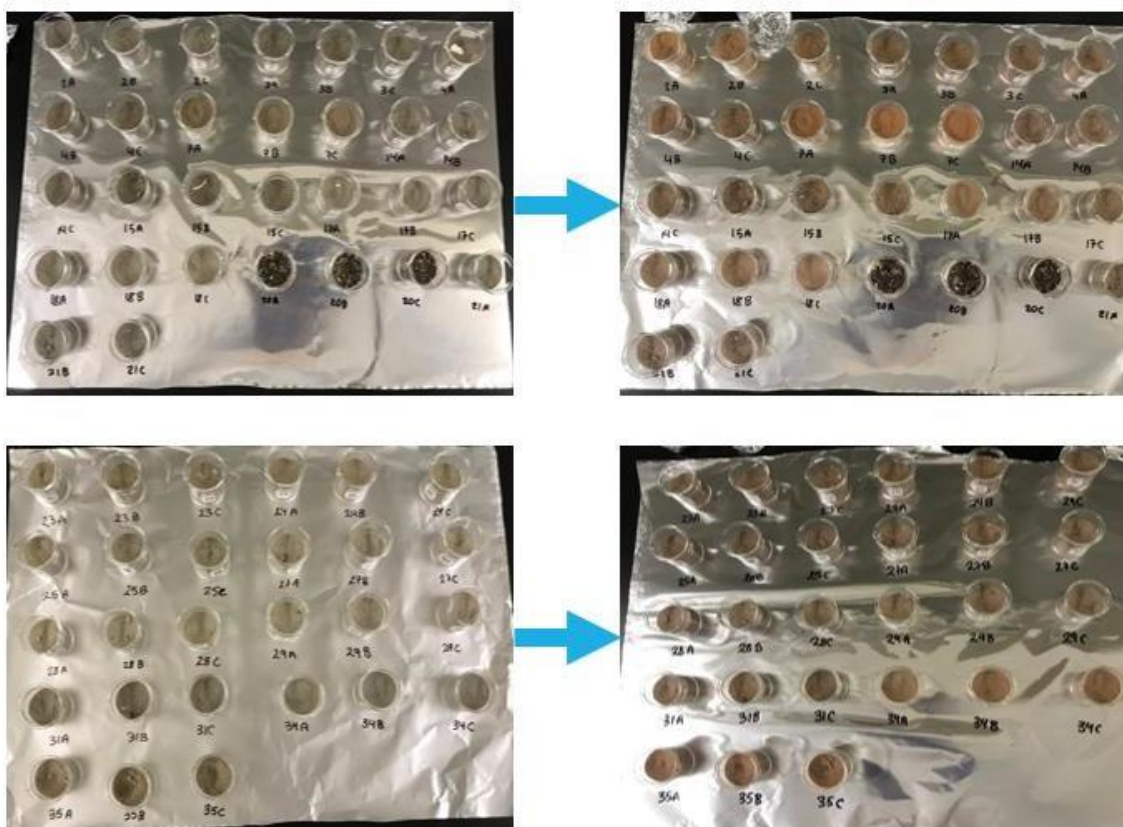


Figure 15. Sediment samples before (left side) and after (right side) loss on ignition method to determine percent organic matter.

The sedimentary OC was collected using an elemental analyzer. Based on the method from (Verardo et al., 1990), samples were ground using a mortar and pestle to form a homogenous powder. Coarse-grained sediment (above 2mm diameter) was excluded since they were too large for elemental analysis. Silver capsules were used to weigh the initial mass (0.5mg-0.7mg), and an acid fumigation was performed by exposing the samples to 37% hydrochloric acid (HCl) to remove any IC. It is significant to note that an acid wash could also potentially remove some OC, which could alter the results. These capsules then placed in an oven overnight at 60 °C and before undergoing analysis.

2.7 Grain Size Analysis

Grain size analysis was conducted on the sediment samples using the protocol derived from Mason (2011). The sediment was first split into pebble/cobble (>4000 μm), gravel (>2000 μm) and fine(<2000 μm) material using mesh sieves. The fraction that was considered <2000 μm was evaluated using a Beckman Coulter's LS 13 320 particle size analyzer at the Bedford Institute of Oceanography. The samples were not treated with acid or hydrogen peroxide since when examining the organic matter in the sediment, there was not an elevated organic content, so it would not interfere with the grain size distribution. The results from the coarse and fine-scale fractions were combined into a full particle size distribution to determine the percentages of the different sediment types.

2.8 Estimation of Total Standing Stock of Organic Carbon

The standing stock of OC was calculated using porosity and dry bulk density. Porosity (Φ) is determined from predicted mud content (dimensionless fraction) from the grain size distribution using the equation (2) derived from Jenkins (2005).

$$\Phi = 0.3805 * C_{mud} + 0.42071 \quad (2)$$

Φ and C_{mud} (mud content) are dimensionless fractions. The equation was derived based on data from the Mississippi-Alabama-Florida shelf, and it is assumed that the equation is not site-specific (Diesing et al., 2017). The equation was also used by Diesing (2017) to examine the standing stock of POC, which emphasizes its validity.

Dry bulk density (p_d) of the sediment was estimated using the porosity and sand grain density ($p_s = 2650 \text{ kg m}^{-3}$) (Diesing et al., 2017; Hunt et al., 2020) found in the equation (3) below:

$$p_d = (1 - \Phi)p_s \quad (3)$$

Estimations of the standing stock of organic carbon (m_{OC}) was derived by multiplying the organic carbon (OC), dry bulk density (p_d), the sediment depth from the Van Veen grab ($d=0.1 \text{ m}$) and area of grid cell ($A= 4 \text{ m}^2$) using the equation (4) below:

$$m_{OC} = OC * p_d * d * A \quad (4)$$

The standing stock of OC per m^2 for each sampling station was averaged to get the average mass of OC per m^2 . Then the average m_{OC} was multiplied by the number of 4 m^2 pixels in the entire study area to determine the total standing stock of OC in the site, assuming that there was no sediment classification map. The total standing stock of OC in the mud/sand sediment type was then estimated by multiplying the average m_{OC} by the number of pixels in the mud/sand area.

3.0 Results

3.1 Random Forest

3.1.1 Variable selection and performance

The random forest algorithm indicated that bathymetry, backscatter, vector ruggedness measure (VRM) and slope were all deemed critical for sediment classification. Figure 16 shows the relative significance of the four variables to prediction accuracy. Backscatter is the most significant variable in predicting sediment type, followed by slope, ruggedness, and bathymetry.

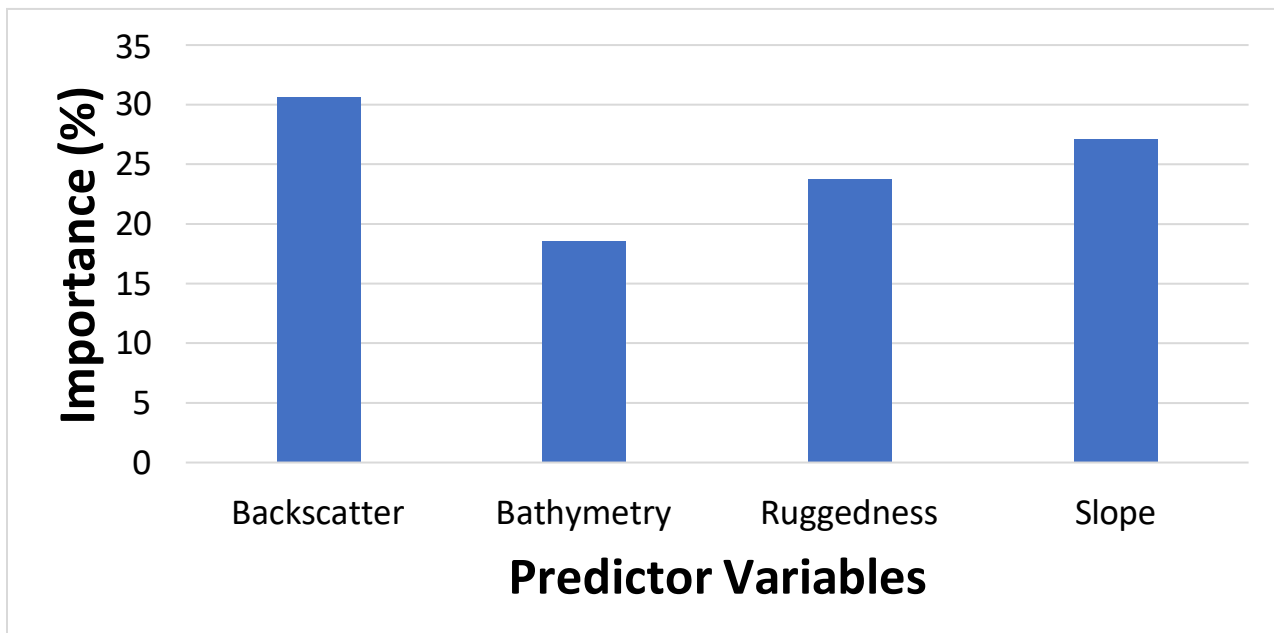


Figure 16. Variable Importance scores. The importance of predictor variables as indicated by the random forest algorithm. The x axis indicates the variables of the final model, the y-axis indicates the relative percent importance. Graph created by Catherine Brennan.

3.1.2 Model Validation

There was 60% MSE in the sediment map random forest model, which indicates extensive error. When examining the accuracy and sensitivity of each sediment class, a confusion matrix can be used to provide insight into how well the forest could predict sediment classification when only using out-of-bag (OOB) features (Figure 17).

	cobble			gravel			mud sand			mud sand gravel		
	cobble	boulder	bedrock	cobble	boulder	ledge	cobble	boulder	bedrock	cobble	boulder	bedrock
cobble/boulder	0	0	0	0	0	0	0	0	0	0	0	0
cobble/boulder/bedrock	0	0	0	1	0	0	0	0	0	0	0	0
gravel/cobble/boulder	0	0	0	0	0	0	2	0	0	0	0	0
gravel/cobble/boulder/bedrock	0	0	2	0	0	0	0	1	0	0	0	0
gravel/ledge	0	0	0	0	0	0	0	0	0	0	0	0
bedrock	0	0	0	0	0	0	0	0	0	0	0	0
mud/sand	0	0	0	0	0	0	7	0	1	0	0	0
mud/sand/cobble/boulder	0	0	0	0	0	0	1	0	0	0	0	0
mud/sand/cobble/boulder/bedrock	0	0	0	0	0	0	0	0	0	0	0	0
mud/sand/gravel	0	0	1	0	0	0	0	0	0	0	0	0
mud/sand/gravel/cobble/boulder	0	0	1	1	0	0	0	0	0	0	0	0
mud/sand/gravel/cobble/boulder/bedrock	0	0	1	0	0	0	0	0	0	0	0	0
mud/sand/bedrock	0	0	0	0	0	0	0	0	0	0	0	0

Figure 17. Confusion Matrix used to determine the sensitivity and accuracy of the map. Chart created by Catherine Brenan.

Accuracy calculations are derived in the equation (5) below:

$$\frac{\text{Number of correct predictions}}{\text{Total number of predictions}} \quad (5)$$

Sensitivity calculations are determined using the equation (6) below:

$$\frac{\text{Number of true positive predictions}}{\text{Total number of all positive events}} \quad (6)$$

For accuracy calculations, the most prominent sediment classes were calculated (Equation 5). Mud/sand/cobble/boulder had the highest accuracy (0.89), then mud/sand (0.88), gravel/cobble/boulder/bedrock (0.74) and gravel/cobble/boulder (0.63) (Figure 18). For sensitivity, all the sediment classes had 0 except for mud/sand, with a 0.88 sensitivity (Equation 6).

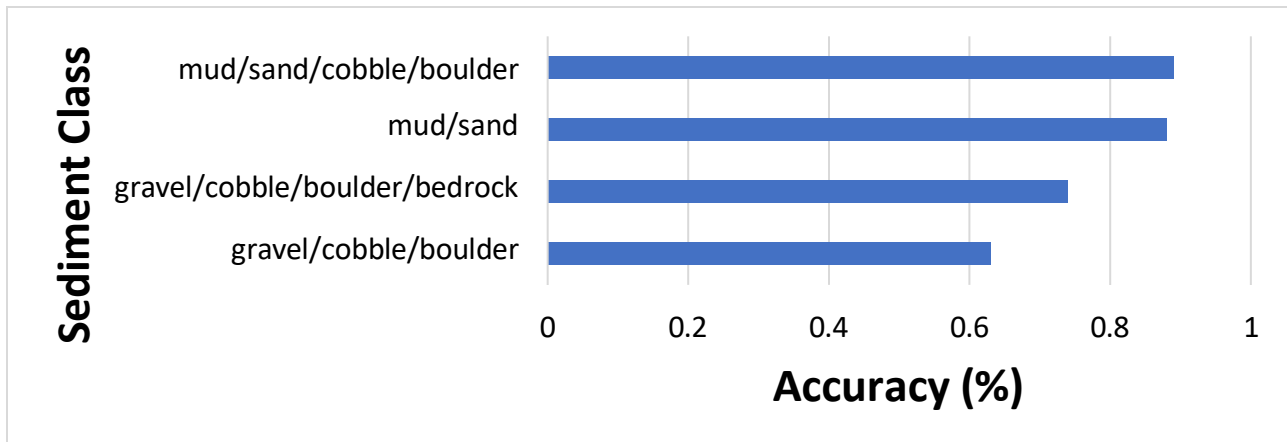


Figure 18. The graph indicates the percent accuracy of the most prominent sediment classes in the sediment classification map. The accuracy can help determine the ability of a random forest algorithm to predict the different substrate types. Chart created by Catherine Brennan

3.2 Mapped Substrate Type

The sediment classification map includes a broad range of sediment types, which suggests a heterogeneous seabed. By analyzing Figures 19 and 20, the most prominent sediment types include gravel/cobble boulder/bedrock, mud/sand, and some gravel/cobble/boulder. There is an extensive amount of mud/sand near the coastal region, in the left of the map and close to the bottom of the study area in the deeper water. Coarse substrates, such as cobble/boulder/bedrock are found throughout the middle of the study area.

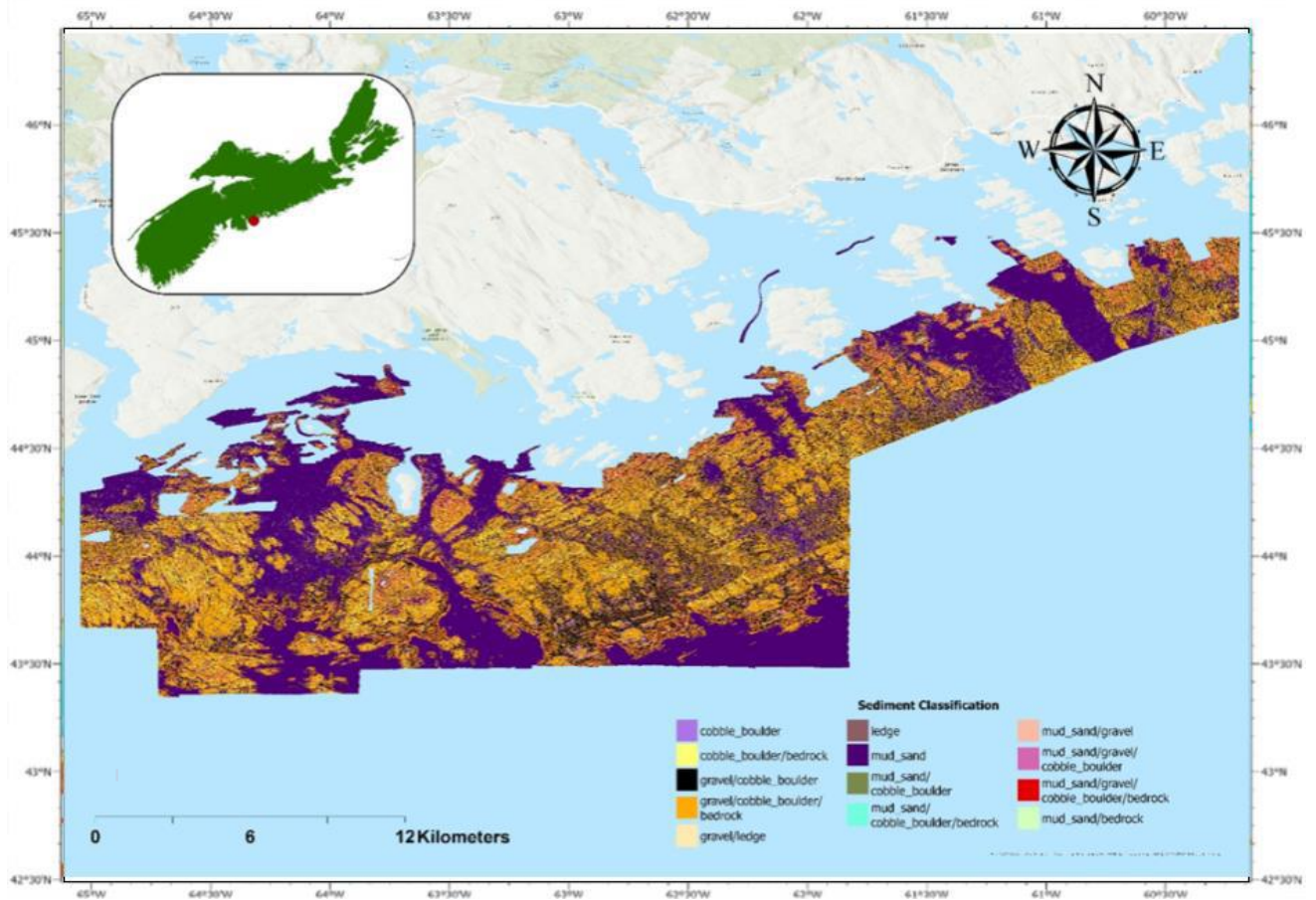


Figure 19. Sediment classification map which was derived using the Forest-Based Classification and Regression tool in ArcGIS Pro. The map was created by Catherine Brennan.

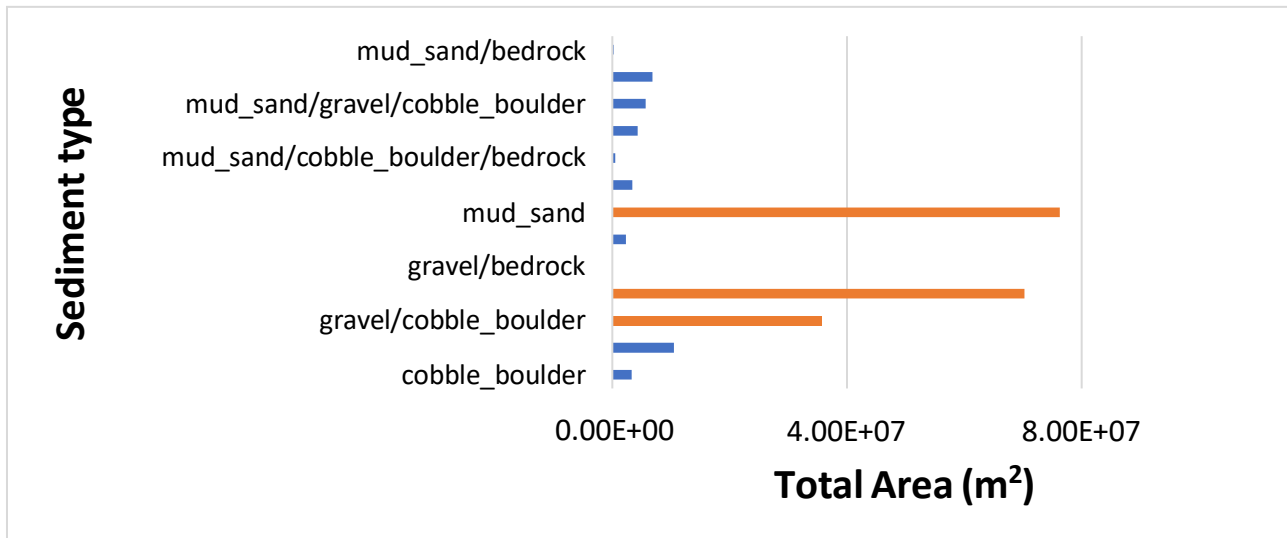


Figure 20. Graph depicting total area (m²) for each sediment type in the substrate classification map. The orange bars indicate the sediment type with the largest total area, which includes mud/sand, gravel/cobble/boulder/bedrock, and gravel/cobble/boulder. Graph created by Catherine Brennan.

3.3 Grab samples

The samples from the Van Veen grab provided grain size and organic carbon measurements at each station (Table 2). Physical samples were only collected in soft sediment allowing most surveys to have a limited amount of coarse grain size (Figure 21). Some coarser substrates (>4000 μm) were found in stations 15 and 17. The grain size classification was derived using the Wentworth scale where >4000 μm indicates boulder, cobble, and pebble and >2000 μm is granule and anything less than 2000 μm is fine sediment (mud and sand). It is important to note that silt and mud were merged into a single mud class. Figure 22 indicates mud (%) and sand (%) amounts in each sample. When examining the graph, most stations have a larger quantity of sand. The exception is survey station seven, with approximately 75% of the sample containing mud.

Table 2. Results from grab samples including grain size and organic carbon measurements.

Table created by Catherine Brennan.

Station	>4000 um (%)	>2000 um (%)	Sand Content (%)	Mud Content (%)	Porosity	Dry Bulk Density (kg/m ³)	Organic Carbon (%)
ES-02	0.27	0.08	54.27	45.38	0.593	1077.6	1.22
ES-03	0.06	0.06	90.80	9.14	0.455	1443.0	0.12
ES-04	0.33	0.01	93.71	5.95	0.443	1475.1	0.13
ES-07	0	0.00	24.42	75.58	0.708	773.0	1.85
ES-15	0.59	0.11	94.60	4.70	0.439	1487.7	0.06
ES-17	2.07	0.30	63.74	33.89	0.550	1193.4	0.10
ES-18	0.60	0.04	80.18	19.18	0.494	1341.7	0.23
ES-19	0.00	0.04	96.69	3.27	0.433	1502.2	0.08
ES-21	0.14	0.10	91.38	8.38	0.453	1450.6	0.06
ES-23	0.08	0.21	93.77	5.93	0.443	1475.3	0.07
ES-25	0.01	0.01	95.43	4.55	0.438	1489.3	0.05
ES-27	0.04	0.05	85.00	14.90	0.477	1384.8	0.07
ES-28	0.00	0.05	85.16	14.80	0.477	1385.9	0.08
ES-29	0.00	0.02	86.72	13.26	0.471	1401.5	0.08
ES-31	21.42	9.97	45.75	22.86	0.508	1304.6	0.83
ES-34	2.15	0.71	52.44	44.70	0.591	1084.4	0.61
ES-35	34.00	0.37	17.33	48.30	0.605	1048.0	0.95

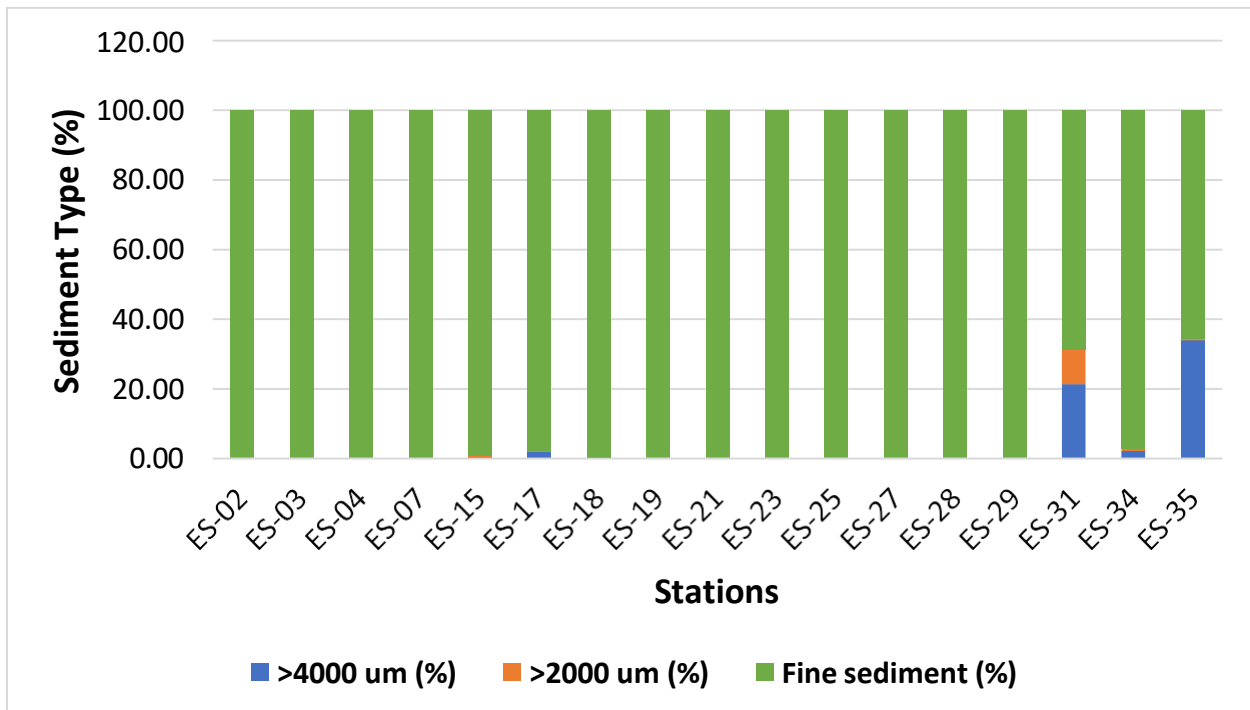


Figure 21. Percentage of sediment type for each sample station. Grain size was determined using the Wentworth scale. Graph created by Catherine Brennan.

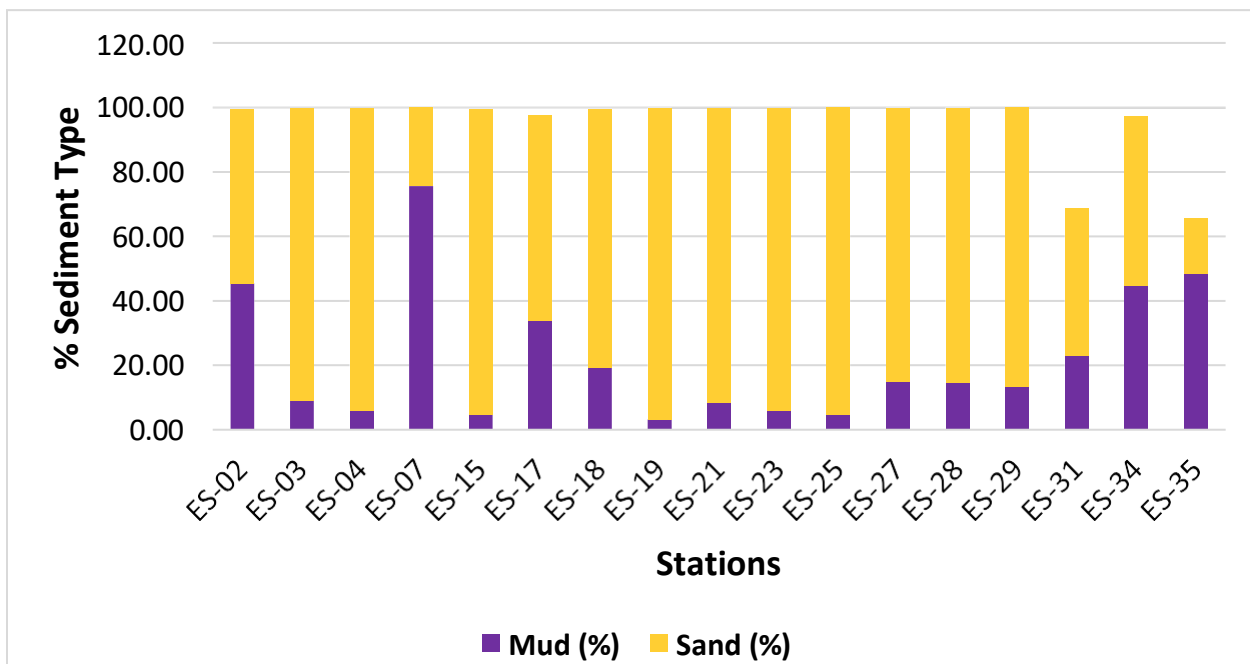


Figure 22. Quantity of mud (%) and sand (%) found for each sample. Graph created by Catherine Brennan

The OC data obtained from the sediment samples indicates that the highest amount of OC is station seven, which is off the coast of little harbour, near the ship harbour ocean inlet (Figure 23). Other areas of high OC include stations 02, 31, 34 and 35, which are near the left centre of the study site, close to lower west Jeddore. When comparing the OC data with other variables, such as backscatter, most of the OC data is found in the dark grey sections of the backscatter, which is softer sediment (Figure 24). Also, when examining the chlorophyll-a concentration (mg/m^3) in surface waters, there was high productivity at station seven which possesses the most substantial amount of OC in the study (Figure 25).

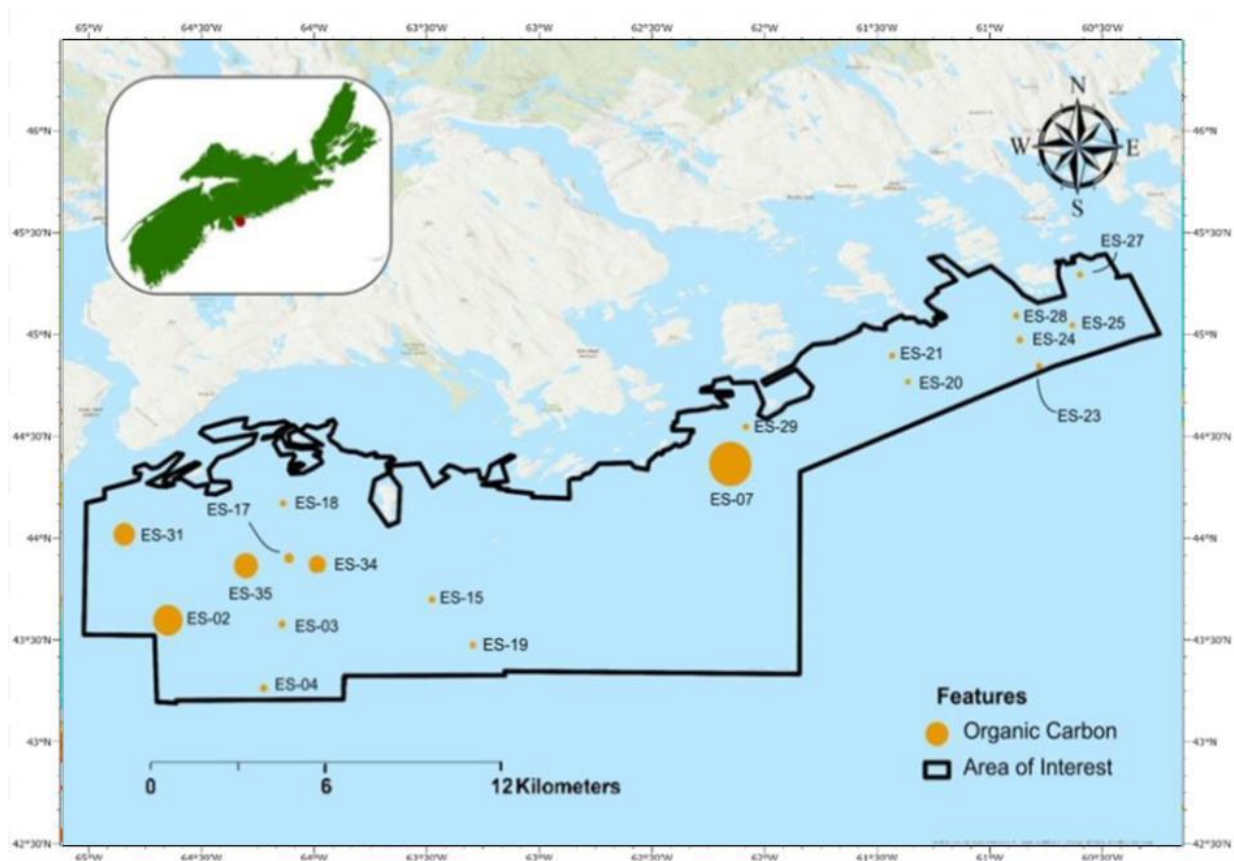


Figure 23. OC data that has been displayed in proportional symbols. Each data point is labeled to their survey station. Map created by Catherine Brennan.

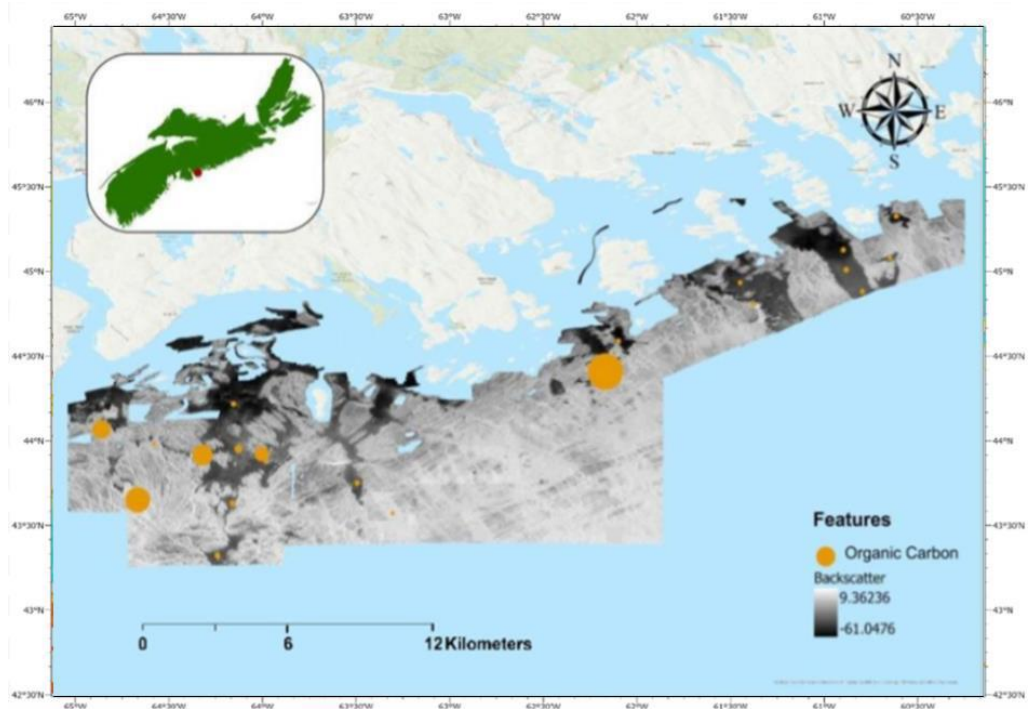


Figure 24. Backscatter overlaid with yellow dots indicating the organic carbon samples. Map created by Catherine Brenan

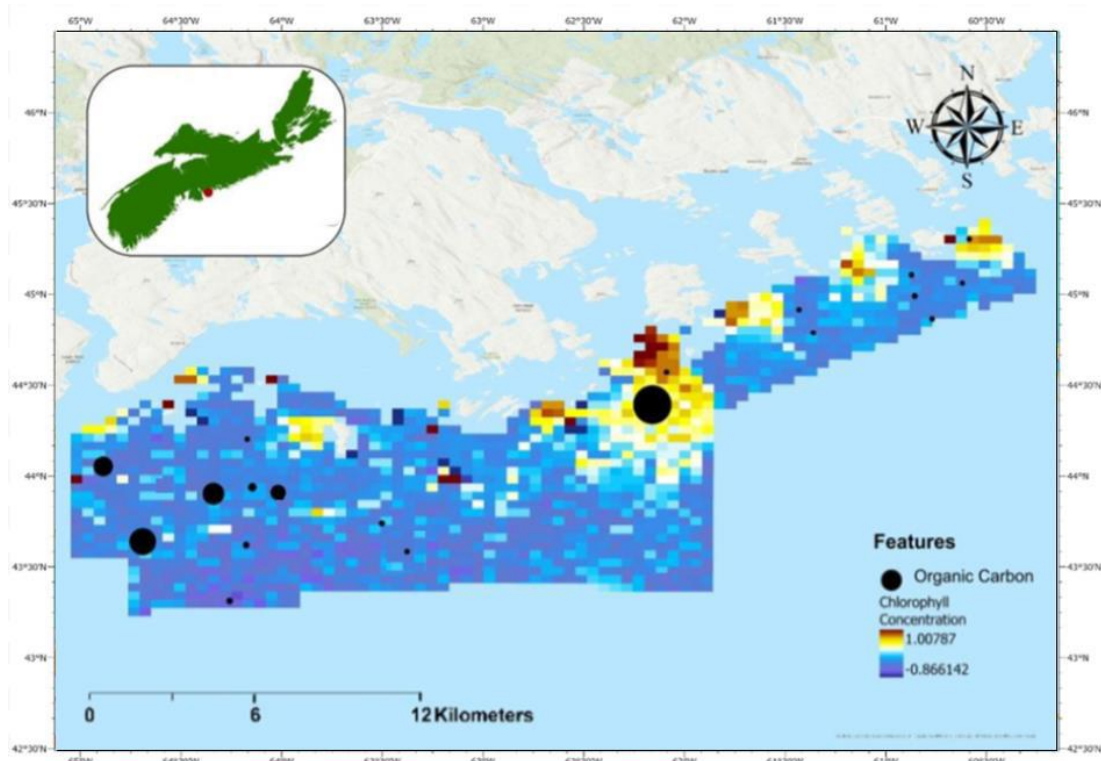


Figure 25. Chlorophyll-a concentration (mg/m^3) which is overlaid with OC measurements. The chlorophyll-a concentration was collected in May 2021 by Sentinel-3 satellite data. Map created by Catherine Brennan

3.4 Relationship between Grain size and Organic Carbon

An ordinal least square regression (OLS) was performed to examine the relationship between OC and percentage grain size composition of sand and mud. OLS analysis between OC and percent sand had all the assumptions met, and the results were statistically significant ($p < 0.001$). Also, there was a substantial negative relationship between OC and percent sand ($R^2 = 0.76$) (Figure 26). The OLS analysis between OC and percent mud had all the assumptions met, and the results were valid ($p < 0.001$). There is a significant positive relationship between OC and percent mud ($R^2 = 0.81$) (Figure 27).

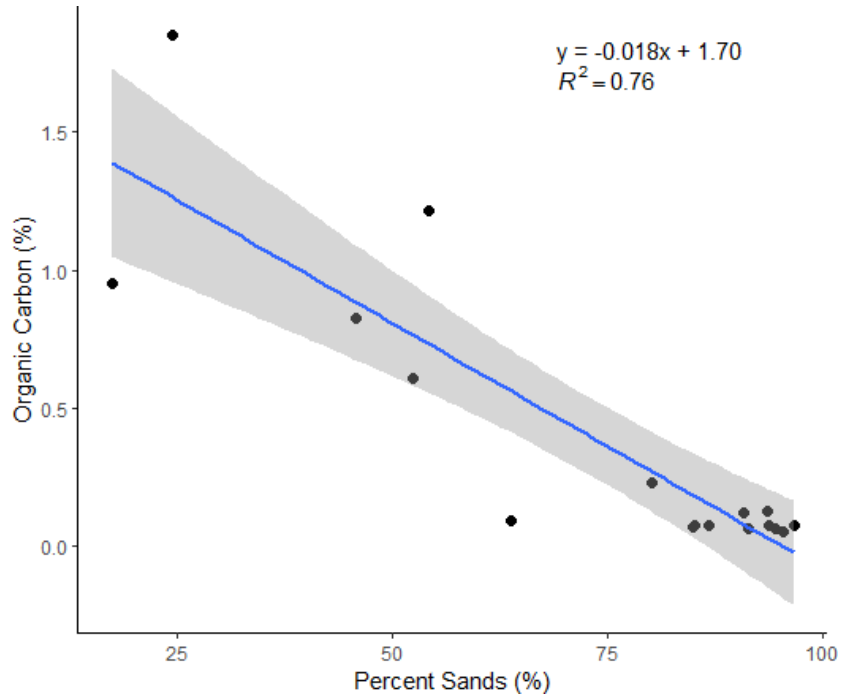


Figure 26. Graph depicting a linear regression between OC and percent sand. The grey area represents a 95 percent confidence interval for the slope of the regression line.

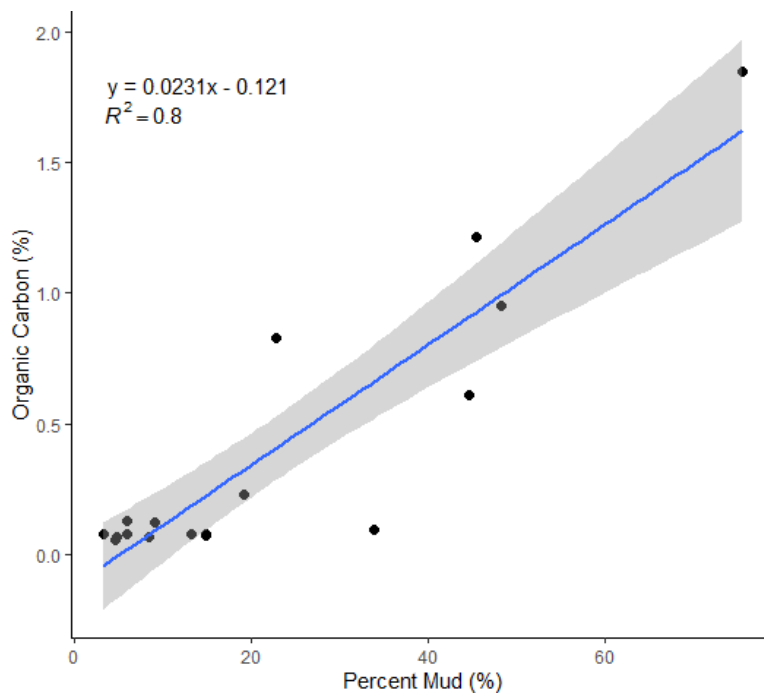


Figure 27. Linear regression graph indicating the relationship between OC and percent mud. The grey area represents a 95 percent confidence interval for the slope of the regression line.

3.5 Organic Carbon in Surficial sediments

After calculating the porosity, dry bulk density and percent OC, the total stock of OC was determined (Table 3). With no sediment map (assuming a homogeneous seafloor across the study area), the OC samples would be scaled up to the entire study area with a total OC stock of 9,133,380 kg/km². Yet, when using the high-resolution substrate map, the estimation for OC changes dramatically to 3,175,522 kg/km². This estimation is assuming no OC in coarse substrata and is only using the area from the mud/sand substrate class.

Table 3. Calculations used to determine the total stock of OC in the mud/sand sediment type and the total stock of OC in the entire study site.

Average Dry Bulk Density (kg/m ³)	Average organic carbon (%)	Average stock of organic carbon (kg/m ²)	Total area of mud/sand sediment class (km ²)	Total stock of organic carbon in mud/sand (kg/km ²)	Total area of study site (km ²)	Total stock of organic carbon in study site (kg/km ²)
772.98 to 1489.27	0.054 to 1.851	32.168 to 572.31	19,072	613,536 to 10,915,548	54,856	1,764,642 to 31,395,107

4.0 Discussion

Through this study, we have described a quantitative spatial model of sediment type in the Eastern Shore islands. Furthermore, we have determined an estimate of OC in the surficial sediments with and without the seabed classification map. The results suggested that the sediment classification map had a substantial amount of error within the model yet still provided insight spatially into the geology of the seabed, indicating the degree of seafloor heterogeneity and complexity in the region. This indicated that we could model sediment type in the benthic environment using multibeam echosounder surveys in the offshore Eastern Shore Islands. Also, the difference in the total stock of OC with and without the substrate map emphasized that high-resolution sediment classification maps can assist in estimating the total standing stock of OC deposits on the seabed in the offshore Eastern Shore Islands.

4.1 Comparison between Sediment Map and Previous Studies in the Eastern Shore Islands

The sediment classification model indicated a high error/low performance, but it captured the correct spatial substrate patterns and showed good agreement with the expert interpretation by eye substrate map derived by the Geological Survey of Canada (King, 2018) (Figure 2). Both included mud content near the coastline, which could signify that the fine sediment is supplied by rivers which form tidal flats and drainage channel deposits (King, 2018). Significant portions of mud were found farther into the study site where the depth was 100 m, which suggested glacial marine mud deposits or sediment transport offshore. One difference between the maps was that bedrock was determined across the study area in the geological survey with some gravel and cobble substrates. In our study, the highest quantity of coarse substrate was gravel/cobble/boulder/bedrock. Our map implied that there was more complexity found within the larger-grained sediment.

Another difference between the maps was that the map developed by the Geological Survey of Canada differentiated between mud and sand and examined the different layers of sediment deposits, such as thin sand over bedrock or thicker glacial marine mud over bedrock. Due to the use of drop camera imagery in this study, the sediment map could not distinguish layers of sediment. Yet, there was an indication of sediment layering when examining the backscatter overlaid by the OC data (figure 24). OC data such as ES-02 was mostly fine sediment, but there was high-intensity backscatter in that location, indicating that there could be penetration of the acoustics through the veneer with possible higher backscatter from the subsurface rock/coarse substrata (Hunt et al. 2021). Further data, such as sediment cores, could help provide new insights on the distribution of surficial sediments.

Another distinction between the sediment map from this study and the previous map is that the geological survey stated that the most extensive substrate is the bedrock derived from land geology. But our study suggested mud and sand had the most considerable area. After examining the difference between both maps, it emphasizes how machine learning models can be very effective at creating sediment maps, yet expert interpretation is still needed to validate the output of the model.

4.2 Factors Controlling Organic Carbon

When examining the grab sample data, samples that had a higher percentage of mud compared to sand had higher amounts of OC (samples 2, 7, 31, 34 and 35). This was further validated in the OLS regression since there was a statistically significant positive relationship between mud content (Figure 27) and OC, and a negative relationship between sand content and OC (Figure 26). Furthermore, this trend agrees with the papers from Lima et al. (2020) and Hunt et al. (2020), which suggest that grain size can act as a proxy to determine the amount of OC in a region. These studies explained that the relationships between OC and sediment composition are due to various mechanisms, such as the sorption of organic matter to mineral surfaces or high primary productivity in a dynamic system, like coastal upwelling. Also, fine sediment often has high amounts of organic matter due to

proximity to terrestrial inputs and sedimentary hydrographic environments of low natural disturbance (Diesing et al. 2017).

Also, the OC survey map indicated that the highest amount of OC collected was at station seven (Figure 23). When comparing the chlorophyll productivity concentration on the surface waters with the OC, there was a positive correlation in survey site seven, with high amounts of primary productivity where there were significant quantities of OC on the seafloor (Figure 25). The high amount of OC and primary productivity could be due to an influx of organic matter from terrestrial inputs and drainage river catchments, which led to localized primary production in surface waters. Further investigation would need to occur to determine the direct source. Other survey sites with large OC, such as stations two and 35, did not show a substantial relationship between primary productivity on the ocean surface and OC on the seabed.

Previous studies have examined carbon quantity on the surface of the oceans by analyzing phytoplankton activity using satellite imagery since there is an assumption that carbon on the surface of the oceans can correlate with areas of high carbon storage (Chase et al., 2022). The observations found in this study counteract the assumption found in Chase et al. (2022) and suggest that there is a relationship between OC on the surface and at the bottom of the seafloor, yet there are still many processes in the pelagic and benthic regions that alter the OC content before it reaches the seabed. This emphasizes that we currently have a poor understanding of the carbon cycle in the oceans and how further research should evaluate the relationship between surface carbon and carbon quantities on the seafloor.

Furthermore, without a sediment map of the seafloor, the OC would be scaled up to the entire study site to estimate standing stocks. This would not precisely represent the OC in the region since the eastern shore islands is heterogeneous seabed with high amounts of coarse substrate like bedrock/cobble/ boulder, which would have a negligible quantity of OC. With the sediment map, the survey samples were found only in the mud/sand substrate type (Figure 21).

This is a more realistic depiction of the storage of OC on the surface of the seafloor and led to a smaller range in the total OC stock. The difference in OC stock suggests that high-resolution sediment classification maps can be valuable in providing accurate representations of the quantity of OC on the seafloor. Also, this study could be scaled up to even broader regions since shelf environments are inherently heterogeneous and therefore obtaining accurate estimates of OC can be challenging (Snelgrove et al., 2018). Carbon studies need to embrace the complexity of the seafloor to determine the coarsest change in carbon cycling due to climate change (Snelgrove et al., 2018).

Also, it is significant to note that the average OC stock of each survey site had high variation which could be due to the small sample size and high resolution of the sediment map. Further observations could provide more consistent values to decrease range and provide a more approximate estimation of average OC stock in the study site.

When examining OC stocks in other studies, such as the work of Diesing et al. (2017), they found that the highest mass of POC was associated with gravelly mud, mud, and sandy mud areas. This correlates with our OLS analysis that areas of increased OC have a high mud content. Furthermore, Diesing et al. (2017) determined that the total standing stock of POC in the top 10 cm of shelf sediment was an average of 434,000 kg/km² in the Northwest European Continental Shelf. Other papers determined an approximate standing stock of OC of 2,0627,000 kg/km² (Smeaton et al., 2019) and 1,144,000 kg/km² (Hunt et al., 2021) found in the fjords of Mainland Scotland. These values emphasize a large amount of variation in OC depending on location. The variation in total stock found in our study is within range of other carbon studies, yet the high variation in our stock could be due to the limited number of carbon samples collected. These substantial ranges between standing stocks of OC suggest how essential it is to examine the relationship between sediment type and OC since it is the substrate that will undergo long-term carbon storage.

4.3 Limitations in the study

Some limitations in the study included a lack of OC survey samples. It is common in spatially mapping carbon studies to have insufficient carbon data due to the inability to collect measurements from a hard substrate. The lack of data heavily restricted the analysis of carbon, leading to some likely errors in estimating OC through the study site. Also, when examining the total organic carbon stock, it is not distributed uniformly across the study area due to variation in response to sediment type and localized hydrographic processes (Burrows et al. 2014). This suggests that maps showing the distribution of OC are important to determine where the carbon hotspots are located within the Eastern Shore Islands. With a large quantity of OC data, a random forest map could have been constructed to determine the standing stock of organic carbon using derived predictor variables. Yet, with the limited OC samples, the interpolation of the points did not make sense spatially.

Also, when examining the sediment map, there was a considerable mean of the squared prediction error. The error could be due to the extensive noise from the backscatter variable, even when reducing the noise through the filter (spatial analysis) tool. The impact of the anomalous cells can be seen in the center-right of the map since it is heavily pixelated. Also, the relationship between backscatter and sediment type can be complex, and other factors could have altered the backscatter, such as environmental characteristics like sediment density and bioturbation from benthic communities (Hunt, 2021). It is also notable to mention that random forest does not estimate spatially explicit uncertainty and only quantifies model uncertainty. This flaw in the algorithm means that if there is a large amount of error within the model from the pixel-based noise, there could still be low uncertainty spatially, suggesting that the model is still sufficient for examining the sediment over the study site.

Another limitation of the sediment map is the DFO drop camera imagery used to differentiate sediment classes. The data provided by DFO did not distinguish between mud and

sand or cobble and boulder. Furthermore, since it was just an image with no ground truth sample like sediment cores, it was not possible to determine the different sediment in the layers, such as a thin layer of mud on top of bedrock. By differentiating the mud and sand substrate, it could provide insight into which fine sediment stores the most carbon in the area. Muddy sediments store high quantities of OC, but they often supply little to the total stock since there in spatially restricted areas and have a low dry bulk density (Diesing, 2017). Sand can often contribute more to the OC stock due to high dry bulk density and widespread occurrence in the study area.

Additionally, numerous variables influence OC quantity, such as oxygen penetration, water temperature, sedimentation rate, disturbance levels and age/transportation times (Smeaton, 2017). These factors were not considered in this study, and it emphasizes the complexity when examining carbon on the seafloor. Using high-resolution sediment classification maps can only explain a fragment of the biogeochemical processes that influence long term carbon storage.

4.4 Future Work

Future work in the Eastern Shore Islands includes more fieldwork to obtain grab samples. Additional grab samples could help refine the conclusions from this study and provide more insight into the correlation between sediment type and how it can predict carbon. More OC data could also help derive a high-resolution OC map, which could determine areas of high OC and low OC within the fine sediment of the study site. Also, benthic-pelagic coupling varies spatially, so by creating a high-resolution map of the distribution of OC, we could understand the dramatic effect that this process has on carbon input to the benthic system.

In addition, the drop camera imagery conducted by DFO occurred in the fall, yet the carbon sampling field work happened in the spring. The change in seasons emphasizes the need for more consistent data collected during all seasons and throughout multiple years since it

could provide a longer timeline and overall average of the change in carbon. Also, sediment traps could be deployed over a long period to measure sedimentation rates. Sedimentation rate data can give information about the depositional environment of marine sediments (Smeaton et al. 2019; Leduc et al., 2023). This information is valuable for carbon storage since it is not only essential to examine the relationship between grain size and OC, but future studies need to also incorporate the sedimentation rates of the seafloor and how quickly new carbon deposits can be stored before oxygenation (Smeaton et al., 2021). Studies have found that sediments deposited under oxic deep-water conditions provide a positive correlation between OC content and sedimentation rate (Stein, 1990). It would be interesting to see if these results correlate with our study site.

Other forms of sampling, such as sediment cores and porewater data, could lead us to develop more questions concerning carbon on the seafloor. Sediment cores allow for radiocarbon dating since they can provide a timeline for past ocean conditions, carbon composition and how it is shifting due to climate change (Magill et al., 2018). Porewater samples are water extracted from the sediment and measure different trace elements, which provides insight into the rate of chemical reactions and their relationship to carbon within the sediment (Smeaton et al. 2019). Furthermore, doing more elemental analysis, such as carbon-to-nitrogen ratios, can indicate the nitrogen limitation of plants and other organisms and identify whether molecules found in the sediment come from land-based or algal plants (Magill et al., 2018).

Also, it is vital to state that assessing carbon processing on the seafloor is a multidisciplinary approach. Geochemists ignore the organisms and focus on quantifying burial, and ecologists follow carbon transfers in the food webs and focus on the growth and biomass of organisms (Middelburg, 2019). These different perspectives can lead to models having different conclusions based on biased approaches. In this study, OC was examined based on a geochemical approach since there was an emphasis on sediment type and grain size analysis. Future work should combine other variables that relate to carbon, such as the relationship

between bioturbating organisms and OC on the seafloor (Lo Giudice Cappelli et al., 2019). Also, adding physical oceanography variables like current, bottom temperature and bottom salinity could help provide a more in-depth understanding of how OC is being processed in the substrate.

5.0 Conclusion

High-resolution sedimentary maps can be essential for targeted seabed management, and marine spatial planners should consider ecosystem functioning like carbon sequestration and storage when determining marine protected areas. Sediment, especially muddy sediment, is a long-term store of carbon and is often vulnerable to human activities, such as bottom trawling leading to GHG emissions from the remineralization of buried carbon (Hunt et al. 2021). Further research should explore high-resolution multibeam echosounder data in determining OC rich hotspots to help support management measures.

In this study, more ground truthing is necessary to create more precise measurements of OC and to further evaluate which sediment type is most significant for OC storage. Despite the limited dataset, sediment classification maps are necessary to improve our understanding of spatial patterns of OC and thus support the idea that marine carbon is a nature-based solution for climate change mitigation.

6.0 References

- Araújo, R. M., Assis, J., Aguillar, R., Airoidi, L., Bárbara, I., Bartsch, I., Bekkby, T., Christie, H., Davoult, D., Derrien-Courtel, S., Fernandez, C., Fredriksen, S., Gevaert, F., Gundersen, H., Le Gal, A., Lévêque, L., Mieszkowska, N., Norderhaug, K. M., Oliveira, P., ... Sousa-Pinto, I. (2016). Status, trends and drivers of kelp forests in Europe: An expert assessment. *Biodiversity and Conservation*, 25(7), 1319–1348. <https://doi.org/10.1007/s10531-016-1141-7>
- Arias-Ortiz, Serrano, O., Masqué, P., Lavery, P. S., Mueller, U., Kendrick, G. A., Rozaimi, M., Esteban, A., Fourqurean, J. W., Marbà, N., Mateo, M. A., Murray, K., Rule, M. J., & Duarte, C. M. (2018). A marine heatwave drives massive losses from the world's largest seagrass carbon stocks. *Nature Climate Change*, 8(4), 338–344. <https://doi.org/10.1038/s41558-018-0096-y>
- Artigas, F., Shin, J. Y., Hobbie, C., Marti-Donati, A., Schäfer, K. V. R., & Pechmann, I. (2015). Long term carbon storage potential and CO₂ sink strength of a restored salt marsh in New Jersey. *Agricultural and Forest Meteorology*, 200, 313–321. <https://doi.org/10.1016/j.agrformet.2014.09.012>
- Atwood, T. B., Witt, A., Mayorga, J., Hammill, E., & Sala, E. (2020). Global Patterns in Marine Sediment Carbon Stocks. *Frontiers in Marine Science*, 7, 165. <https://doi.org/10.3389/fmars.2020.00165>
- Bianchi, Miyazawa, M. A. do P., Oliveira, E. L. de(Instituto A. do P., & Pavan, M. A. A. do P. (2008). Relationship between the mass of organic matter and carbon in soil. *Brazilian Archives of Biology and Technology*, 51(2), 263–269. <https://doi.org/10.1590/S1516-89132008000200005>
- Bianchi, T. S., Brown, C. J., Snelgrove, P. V. R., Stanley, R. R. E., Cote, D., & Morris, C. (2023). Benthic Invertebrates on the Move: A Tale of Ocean Warming and Sediment Carbon Storage. *Limnology and Oceanography Bulletin*, 32(1), 1–5. <https://doi.org/10.1002/lob.10544>

- Bradley, J. A., Hülse, D., LaRowe, D. E., & Arndt, S. (2022). Transfer efficiency of organic carbon in marine sediments. *Nature Communications*, *13*(1), 7297. <https://doi.org/10.1038/s41467-022-35112-9>
- Brown, C. J., Smith, S. J., Lawton, P., & Anderson, J. T. (2011). Benthic habitat mapping: A review of progress towards improved understanding of the spatial ecology of the seafloor using acoustic techniques. *Estuarine, Coastal and Shelf Science*, *92*(3), 502–520. <https://doi.org/10.1016/j.ecss.2011.02.007>
- Buhl-Mortensen, P., Lecours, V., & Brown, C. J. (2021). Editorial: Seafloor Mapping of the Atlantic Ocean. *Frontiers in Marine Science*, *8*, 721602. <https://doi.org/10.3389/fmars.2021.721602>
- Burrows, M., Kamenos, N., Hughes, D., Stahl, H., Howe, J., & Tett, P. (2014). *Assessment of carbon budgets and potential blue carbon stores in Scotland's coastal and marine environment. Scottish Natural Heritage Commissioned Report*. (Vol. 1–761). http://www.snh.org.uk/pdfs/publications/commissioned_reports/761.pdf
- Chase, A. P., Boss, E. S., Haëntjens, N., Culhane, E., Roesler, C., & Karp-Boss, L. (2022). Plankton Imagery Data Inform Satellite-Based Estimates of Diatom Carbon. *Geophysical Research Letters*, *49*(13). <https://doi.org/10.1029/2022GL098076>
- Claustre, Legendre, L., Boyd, P. W., & Levy, M. (2021). The Oceans' Biological Carbon Pumps: Framework for a Research Observational Community Approach. *Frontiers in Marine Science*, *8*. <https://doi.org/10.3389/fmars.2021.780052>
- Diesing, M., Kröger, S., Parker, R., Jenkins, C., Mason, C., & Weston, K. (2017). Predicting the standing stock of organic carbon in surface sediments of the North–West European continental shelf. *Biogeochemistry*, *135*(1–2), 183–200. <https://doi.org/10.1007/s10533-017-0310-4>
- Diesing, M., Thorsnes, T., & Bjarnadóttir, L. R. (2021). Organic carbon densities and accumulation rates in surface sediments of the North Sea and Skagerrak. *Biogeosciences*, *18*(6), 2139–2160. <https://doi.org/10.5194/bg-18-2139-2021>

- Eleftheriou, A. and McIntyre, A. (2005) *Methods for Study of Marine Benthos*. 3rd Edition, Vol. 1004, Blackwell Science, Hoboken, NJ.
<https://doi.org/10.1002/9780470995129>
- Feng, T., Stanley, R. R. E., Wu, Y., Kenchington, E., Xu, J., & Horne, E. (2022). A High-Resolution 3-D Circulation Model in a Complex Archipelago on the Coastal Scotian Shelf. *Journal of Geophysical Research: Oceans*, 127(3). <https://doi.org/10.1029/2021JC017791>
- Fennel, K., Alin, S., Barbero, L., Evans, W., Bourgeois, T., Cooley, S., Dunne, J., Feely, R. A., Hernandez-Ayon, J. M., Hu, X., Lohrenz, S., Muller-Karger, F., Najjar, R., Robbins, L., Shadwick, E., Siedlecki, S., Steiner, N., Sutton, A., Turk, D., ... Wang, Z. A. (2019). Carbon cycling in the North American coastal ocean: A synthesis. *Biogeosciences*, 16(6), 1281–1304. <https://doi.org/10.5194/bg-16-1281-2019>
- Fourqurean, J. W., Duarte, C. M., Kennedy, H., Marbà, N., Holmer, M., Mateo, M. A., Apostolaki, E. T., Kendrick, G. A., Krause-Jensen, D., McGlathery, K. J., & Serrano, O. (2012). Seagrass ecosystems as a globally significant carbon stock. *Nature Geoscience*, 5(7), 505–509.
<https://doi.org/10.1038/ngeo1477>
- Galvez, D. S., Papenmeier, S., Sander, L., Bartholomä, A., & Wiltshire, K. H. (2022). Ensemble mapping as an alternative to baseline seafloor sediment mapping and monitoring. *Geo-Marine Letters*, 42(3), 11. <https://doi.org/10.1007/s00367-022-00734-x>
- Gregory, R., & Anderson, J. (1997). Substrate selection and use of protective cover by juvenile Atlantic cod *Gadus morhua* in inshore waters of Newfoundland. *Marine Ecology Progress Series*, 146, 9–20. <https://doi.org/10.3354/meps146009>
- Hilmi, N., Chami, R., Sutherland, M. D., Hall-Spencer, J. M., Lebleu, L., Benitez, M. B., & Levin, L. A. (2021). The Role of Blue Carbon in Climate Change Mitigation and Carbon Stock Conservation. *Frontiers in Climate*, 3, 710546.
<https://doi.org/10.3389/fclim.2021.710546>
- Howard, P. J. A., & Howard, D. M. (1990). Use of organic carbon and loss-on-ignition to estimate soil organic matter in different soil types and horizons. *Biology and Fertility of Soils*, 9(4), 306–310. <https://doi.org/10.1007/BF00634106>

- Hunt, C. A., Demšar, U., Marchant, B., Dove, D., & Austin, W. E. N. (2021). Sounding Out the Carbon: The Potential of Acoustic Backscatter Data to Yield Improved Spatial Predictions of Organic Carbon in Marine Sediments. *Frontiers in Marine Science*, 8, 756400. <https://doi.org/10.3389/fmars.2021.756400>
- Hunt, C., Demšar, U., Dove, D., Smeaton, C., Cooper, R., & Austin, W. E. N. (2020). Quantifying Marine Sedimentary Carbon: A New Spatial Analysis Approach Using Seafloor Acoustics, Imagery, and Ground-Truthing Data in Scotland. *Frontiers in Marine Science*, 7, 588. <https://doi.org/10.3389/fmars.2020.00588>
- Janowski, L., Madricardo, F., Fogarin, S., Kruss, A., Molinaroli, E., Kubowicz-Grajewska, A., & Tegowski, J. (2020). Spatial and Temporal Changes of Tidal Inlet Using Object-Based Image Analysis of Multibeam Echosounder Measurements: A Case from the Lagoon of Venice, Italy. *Remote Sensing*, 12(13), 2117. <https://doi.org/10.3390/rs12132117>
- Jeffery, N.W., Heaslip, S.G., Stevens, L.A., and Stanley, R.R.E. 2020. Biophysical and Ecological Overview of the Eastern Shore Islands Area of Interest (AOI). DFO Can. Sci. Advis. Sec. Res. Doc. 2019/025. xiii + 138 p.
- Jenkins, C.J., 2005, Summary of the onCALCULATION methods used in dbSEABED, in: Buczkowski, B.J., Reid, J.A., Jenkins, C.J., Reid, J.M., Williams, S.J., and Flocks, J.G., 2006, usSEABED: Gulf of Mexico and Caribbean (Puerto Rico and U.S. Virgin Islands) Offshore Surficial Sediment Data Release: U.S. Geological Survey Data Series 146, version 1.0. Online at <http://pubs.usgs.gov/ds/2006/146/> King, E. L. (2018). *Surficial geology and features of the inner shelf of eastern shore, offshore Nova Scotia* (No. 8375; p. 8375). <https://doi.org/10.4095/308454>
- LaRowe, D. E., Arndt, S., Bradley, J. A., Estes, E. R., Hoarfrost, A., Lang, S. Q., Lloyd, K. G., Mahmoudi, N., Orsi, W. D., Shah Walter, S. R., Steen, A. D., & Zhao, R. (2020). The fate of organic carbon in marine sediments—New insights from recent data and analysis. *Earth-Science Reviews*, 204, 103146. <https://doi.org/10.1016/j.earscirev.2020.103146>
- Leduc, Michèle et al. “A Multi-Approach Inventory of the Blue Carbon Stocks of Posidonia Oceanica Seagrass Meadows: Large Scale Application in Calvi Bay (Corsica, NW Mediterranean).” *Marine environmental research* 183 (2023): 105847–105847. Web.

Legge, O., Johnson, M., Hicks, N., Jickells, T., Diesing, M., Aldridge, J., Andrews, J., Artioli, Y.,
Bakker, D. C. E., Burrows, M. T., Carr, N., Cripps, G., Felgate, S. L., Fernand, L.,

- Greenwood, N., Hartman, S., Kröger, S., Lessin, G., Mahaffey, C., ... Williamson, P. (2020). Carbon on the Northwest European Shelf: Contemporary Budget and Future Influences. *Frontiers in Marine Science*, 7, 143. <https://doi.org/10.3389/fmars.2020.00143>
- Lima, M. do A. C., Ward, R. D., & Joyce, C. B. (2020). Environmental drivers of sediment carbon storage in temperate seagrass meadows. *Hydrobiologia*, 847(7), 1773–1792. <https://doi.org/10.1007/s10750-019-04153-5>
- Lo Giudice Cappelli, Clarke, J. L., Smeaton, C., Davidson, K., & Austin, W. E. N. (2019). Organic-carbon-rich sediments: benthic foraminifera as bio-indicators of depositional environments. *Biogeosciences*, 16(21), 4183–4199. <https://doi.org/10.5194/bg-16-4183-2019>
- Magill, Clayton R et al. “Transient Hydrodynamic Effects Influence Organic Carbon Signatures in Marine Sediments.” *Nature communications* 9.1 (2018): 4690–8. Web.
- Mayer, L., Jakobsson, M., Allen, G., Dorschel, B., Falconer, R., Ferrini, V., Lamarche, G., Snaith, H., & Weatherall, P. (2018). The Nippon Foundation—GEBCO Seabed 2030 Project: The Quest to See the World’s Oceans Completely Mapped by 2030. *Geosciences*, 8(2), 63. <https://doi.org/10.3390/geosciences8020063>
- Misiuk, B., Diesing, M., Aitken, A., Brown, C. J., Edinger, E. N., & Bell, T. (2019). A Spatially Explicit Comparison of Quantitative and Categorical Modelling Approaches for Mapping Seabed Sediments Using Random Forest. *Geosciences*, 9(6), 254. <https://doi.org/10.3390/geosciences9060254>
- Najjar, R. G., Herrmann, M., Alexander, R., Boyer, E. W., Burdige, D. J., Butman, D., Cai, W. -J., Canuel, E. A., Chen, R. F., Friedrichs, M. A. M., Feagin, R. A., Griffith, P. C., Hinson, A. L., Holmquist, J. R., Hu, X., Kemp, W. M., Kroeger, K. D., Mannino, A., McCallister, S. L., ... Zimmerman, R. C. (2018). Carbon Budget of Tidal Wetlands, Estuaries, and Shelf Waters of Eastern North America. *Global Biogeochemical Cycles*, 32(3), 389–416. <https://doi.org/10.1002/2017GB005790>
- Nellemann, C., & GRID--Arendal (Eds.). (2009). *Blue carbon: The role of healthy oceans in binding carbon: a rapid response assessment*. GRID-Arendal.

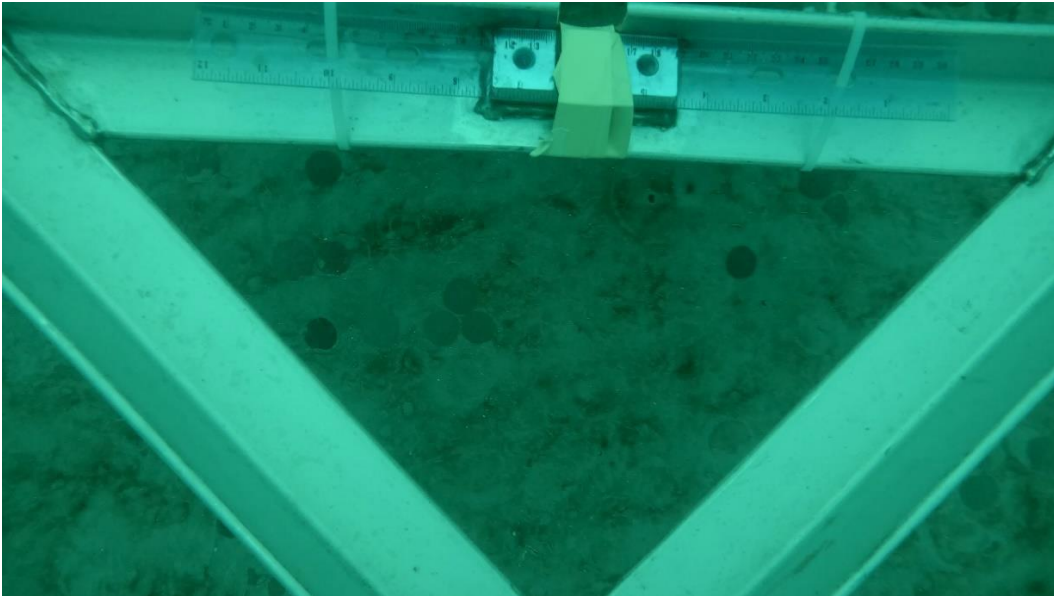
- Proudfoot, B., Devillers, R., Brown, C. J., Edinger, E., & Copeland, A. (2020). Seafloor mapping to support conservation planning in an ecologically unique fjord in Newfoundland and Labrador, Canada. *Journal of Coastal Conservation*, 24(3), 36.
<https://doi.org/10.1007/s11852-020-00746-8>
- Sanders, C. J., Maher, D. T., Tait, D. R., Williams, D., Holloway, C., Sippo, J. Z., & Santos, I. R. (2016). Are global mangrove carbon stocks driven by rainfall?: Mangrove Carbon Stocks. *Journal of Geophysical Research: Biogeosciences*, 121(10), 2600–2609.
<https://doi.org/10.1002/2016JG003510>
- Sarmiento, & Gruber, N. (2006). Ocean biogeochemical dynamics. Princeton University Press.
- Smeaton, C., & Austin, W. E. N. (2019). Where's the Carbon: Exploring the Spatial Heterogeneity of Sedimentary Carbon in Mid-Latitude Fjords. *Frontiers in Earth Science*, 7, 269.
<https://doi.org/10.3389/feart.2019.00269>
- Smeaton, C., Yang, H., & Austin, W. E. N. (2021). Carbon burial in the mid-latitude fjords of Scotland. *Marine Geology*, 441, 106618. <https://doi.org/10.1016/j.margeo.2021.106618>
- Snelgrove, P. V. R., Soetaert, K., Solan, M., Thrush, S., Wei, C.-L., Danovaro, R., Fulweiler, R. W., Kitazato, H., Ingole, B., Norkko, A., Parkes, R. J., & Volkenborn, N. (2018). Global Carbon Cycling on a Heterogeneous Seafloor. *Trends in Ecology & Evolution*, 33(2), 96–105.
<https://doi.org/10.1016/j.tree.2017.11.004>
- Statistics Canada. (2018, September 17). *Thematic Map*. Statistics Canada: Canada's national statistical agency / Statistique Canada : Organisme statistique national du Canada. Retrieved March 25, 2023, from <https://www150.statcan.gc.ca/n1/pub/92-195-x/2011001/other-autre/theme/def-eng.htm>
- Stein, R. (1990). Organic carbon content/sedimentation rate relationship and its paleoenvironmental significance for marine sediments. *Geo-Marine Letters*, 10(1), 37–44. <https://doi.org/10.1007/BF02431020>
- Turnewitsch, R., Dale, A., Lahajnar, N., Lampitt, R. S., & Sakamoto, K. (2017). Can neap-spring tidal cycles modulate biogeochemical fluxes in the abyssal near-seafloor water column? *Progress in Oceanography*, 154, 1–24. <https://doi.org/10.1016/j.pocean.2017.04.006>

- Verardo, D. J., Froelich, P. N., & McIntyre, A. (1990). Determination of organic carbon and nitrogen in marine sediments using the Carlo Erba NA-1500 analyzer. *Deep Sea Research Part A. Oceanographic Research Papers*, 37(1), 157–165. [https://doi.org/10.1016/0198-0149\(90\)90034-S](https://doi.org/10.1016/0198-0149(90)90034-S)
- Wölfel, A.-C., Snaith, H., Amirebrahimi, S., Devey, C. W., Dorschel, B., Ferrini, V., Huvenne, V. A. I., Jakobsson, M., Jencks, J., Johnston, G., Lamarche, G., Mayer, L., Millar, D., Pedersen, T. H., Picard, K., Reitz, A., Schmitt, T., Visbeck, M., Weatherall, P., & Wigley, R. (2019). Seafloor Mapping – The Challenge of a Truly Global Ocean Bathymetry. *Frontiers in Marine Science*, 6, 283. <https://doi.org/10.3389/fmars.2019.00283>

7.0 Appendix

Appendix I: Drop Camera Imagery

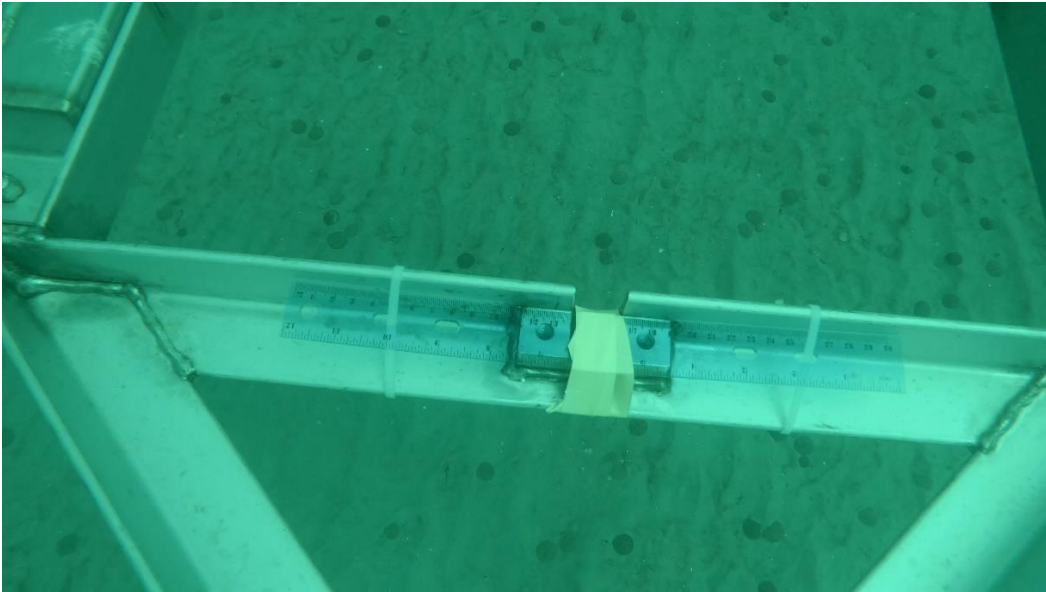
ES-19



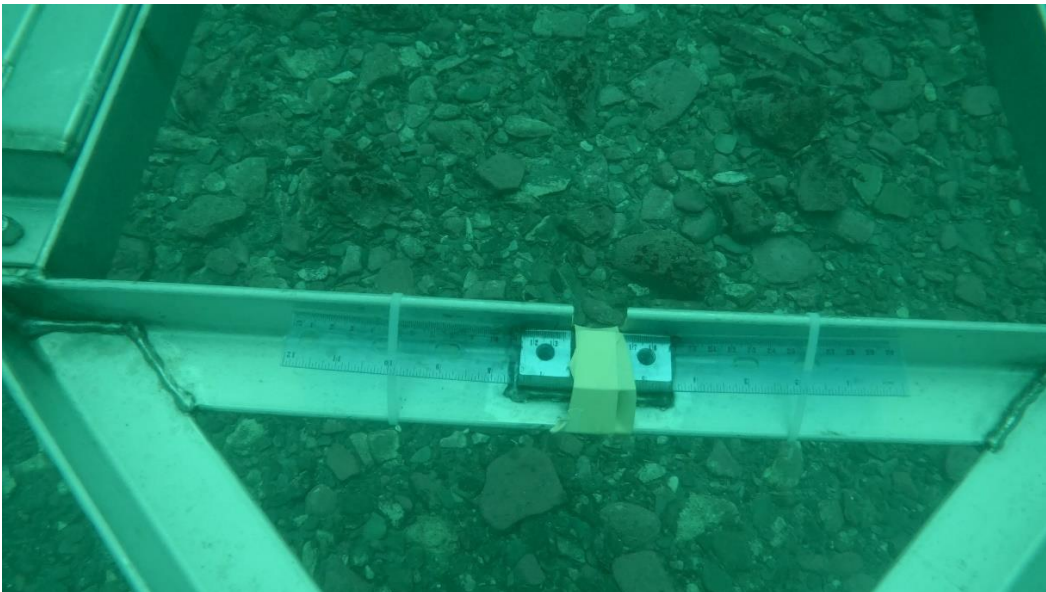
ES-20



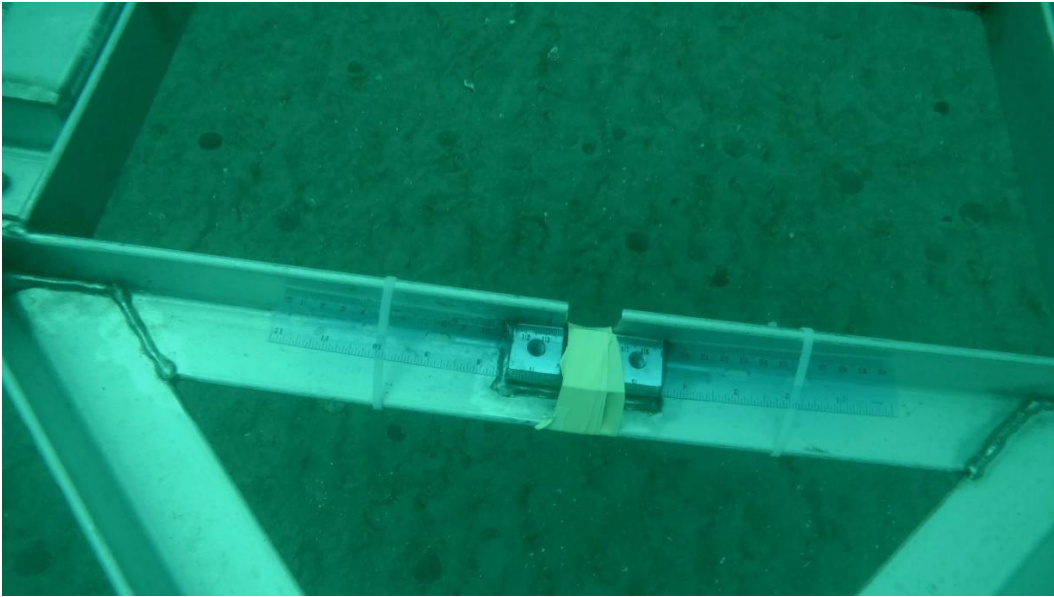
ES-21



ES-22



ES-23



ES-24



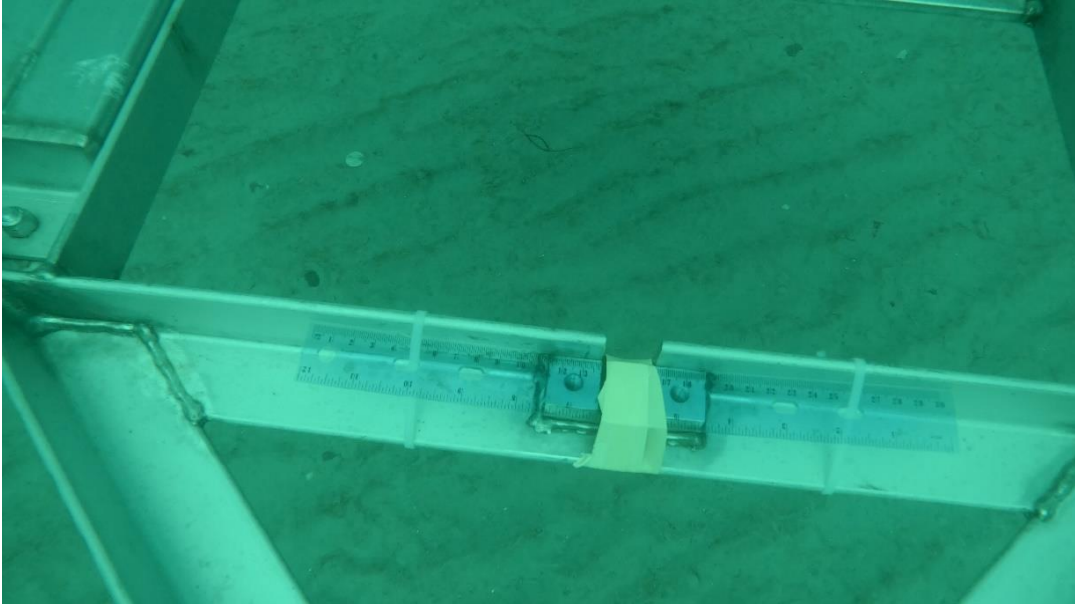
ES-25



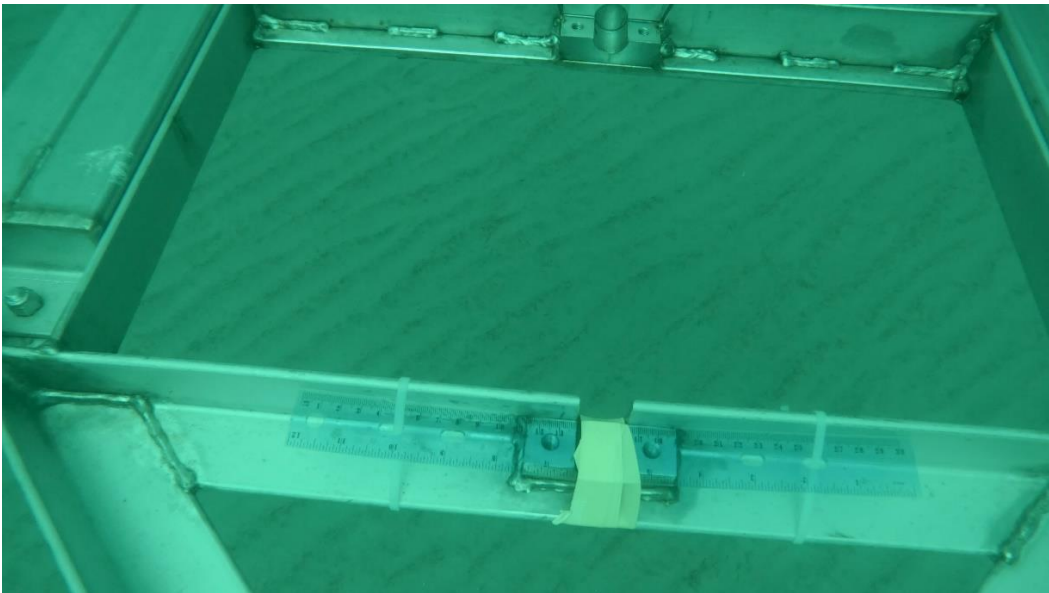
ES-26



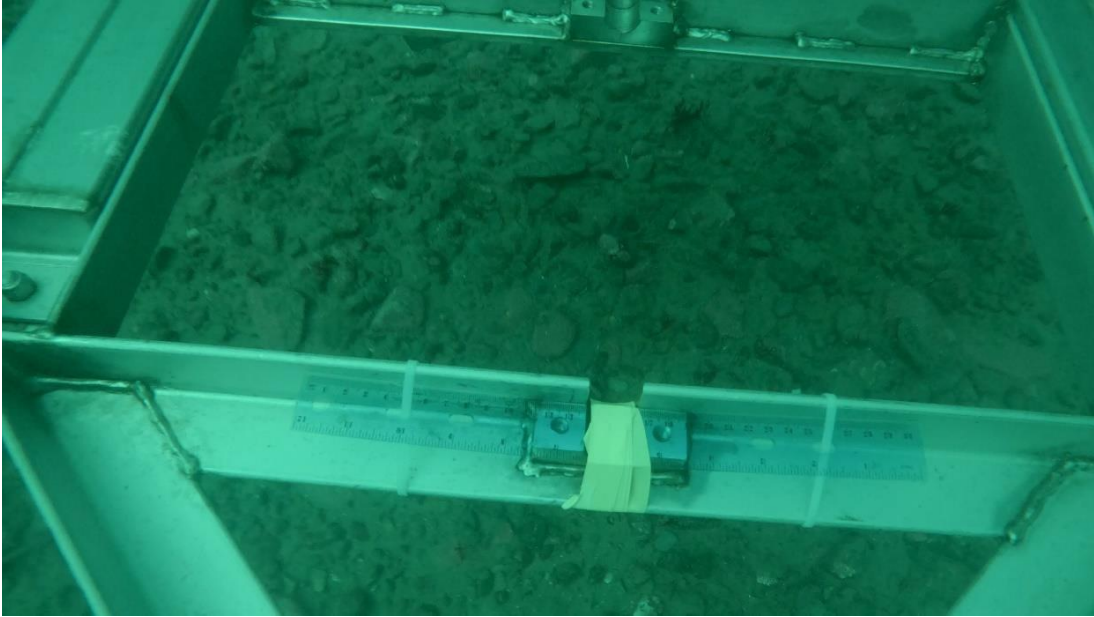
ES-28



ES-29



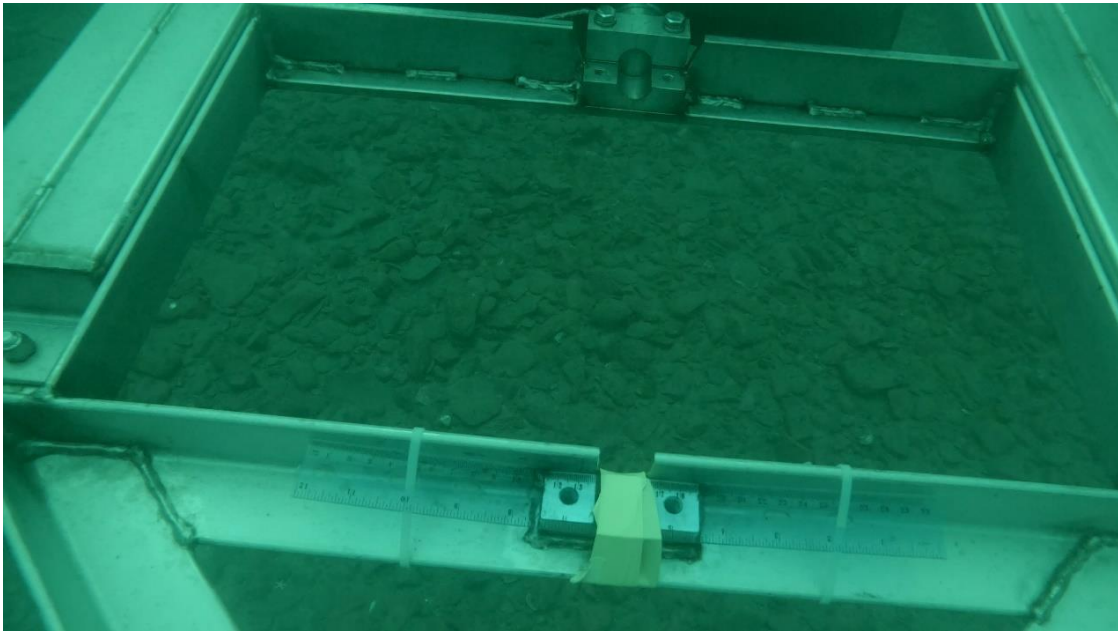
ES-30



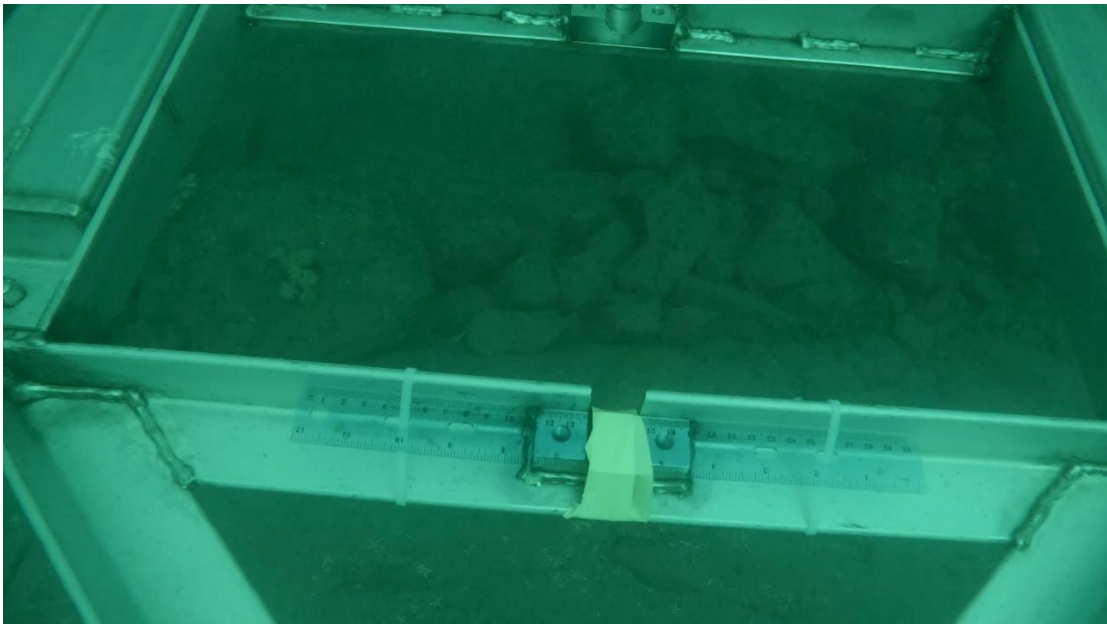
ES-31



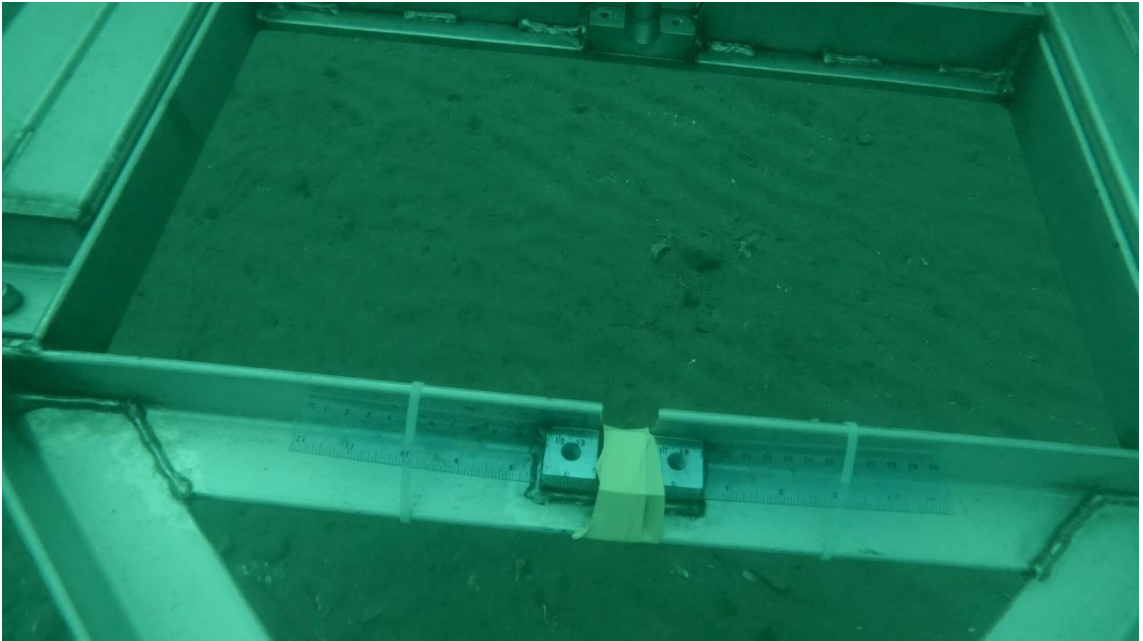
ES-32



ES-33



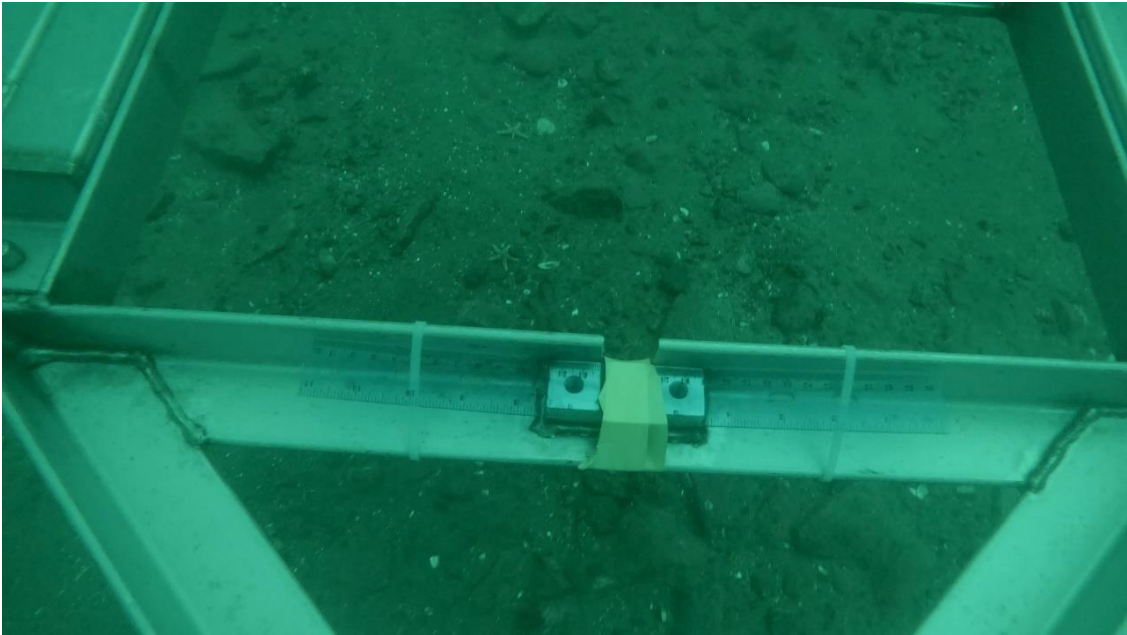
ES-34



ES-35



ES-36



Appendix II: Sediment classification table



Honours_data.xls